Mathematical Biosciences and Engineering

http://www.aimspress.com/journal/MBE

MBE, 18(3): 2033–2076.
DOI: 10.3934/mbe.2021106
Received: 12 December 2020
Accepted: 01 February 2021
Published: 02 March 2021

Review

Detection of glaucoma using retinal fundus images: A comprehensive review

Amsa Shabbir[1], Aqsa Rasheed[1], Huma Shehraz[1], Aliya Saleem[1], Bushra Zafar[2], Muhammad Sajid[3], Nouman Ali[1,*], Saadat Hanif Dar[1] and Tehmina Shehryar[1]

[1] Department of Software Engineering, Mirpur University of Science and Technology (MUST), Mirpur- AJK 10250, Pakistan

[2] Department of Computer Science, Government College University, Faisalabad 38000, Pakistan

[3] Department of Electrical Engineering, Mirpur University of Science and Technology (MUST), Mirpur- AJK 10250, Pakistan

* **Correspondence:** Email: Nouman.se@must.edu.pk; Tel: 0321-9806098.

Abstract: Content-based image analysis and computer vision techniques are used in various health-care systems to detect the diseases. The abnormalities in a human eye are detected through fundus images captured through a fundus camera. Among eye diseases, glaucoma is considered as the second leading case that can result in neurodegeneration illness. The inappropriate intraocular pressure within the human eye is reported as the main cause of this disease. There are no symptoms of glaucoma at earlier stages and if the disease remains unrectified then it can lead to complete blindness. The early diagnosis of glaucoma can prevent permanent loss of vision. Manual examination of human eye is a possible solution however it is dependant on human efforts. The automatic detection of glaucoma by using a combination of image processing, artificial intelligence and computer vision can help to prevent and detect this disease. In this review article, we aim to present a comprehensive review about the various types of glaucoma, causes of glaucoma, the details about the possible treatment, details about the publicly available image benchmarks, performance metrics, and various approaches based on digital image processing, computer vision, and deep learning. The review article presents a detailed study of various published research models that aim to detect glaucoma from low-level feature extraction to recent trends based on deep learning. The pros and cons of each approach are discussed in detail and tabular representations are used to summarize the results of each category. We report our findings and provide possible future research directions to detect glaucoma in conclusion.

Keywords: Medical image processing; computers in medicine; CAD for detection of glaucoma; optic disc abnormalities; retina images; fundus images; review on detection of glaucoma; computer vision techniques to detect glaucoma

1. Introduction

Content-based image analysis is applied in different applications of computer vision and digital images are a major part of multimedia data [1]. In last few decades, significant research is performed on different applications of medical image analysis. The main aim of research in medical image analysis is to assist the doctors to detect diseases on the basis of image contents [2, 3]. Glaucoma is a persistent eye disorder that gradually damages the optic nerve. It is a neurodegeneration illness and contemplates as a reason for blindness. As debasement of nerves is irrevocable action hence it results in permanent loss of vision [3,4]. Numerous research studies have been performed to estimate the number of affected people with this chronic disease [5–7]. Glaucoma is declared as the second leading cause of the loss of sight [8, 9]. Results indicate an estimate of 60 million people suffered from glaucoma in 2010, while the number will be increased to approximately 80 million by 2020 [9]. Glaucoma causes irrevocable vision damage due to elevated Intraocular Pressure (IOP) and optic nerve damage [10]. Glaucoma is commonly referred to as "hushed burglar of vision" since the symptoms at an early stage of glaucoma are not explicitly defined and are hard to quantify. If the succession of glaucoma is not stopped at the initial stages it results in the severe demolition of the optic nerve and as a consequence, it will lead to incurable blindness [11]. It is necessary to detect glaucoma at an early stage due to following facts:

1. There are no perceptible indications in its preliminary stages.
2. It is a severe disorder as the damage it causes is irremediable.
3. It leads to perpetual loss of sight if not cured promptly.
4. There is no prophylactic treatment for glaucoma, but it is possible to avoid blindness by detecting, treating and managing glaucoma at an initial stage [12]. The list of abbreviations used in this paper are shown in the Table 1.

Computer-Aided Diagnosis(CAD) helps in the rehabilitation of the affected eyes of the disease. Numerous research studies have been performed on fundus images to detect glaucoma at an early phase and to avoid any severe damages. Glaucoma alludes to a group of conditions and states characterized by the variations in the retinal nerve fiber cushion and nervous optics head leading to reduced vision and imparity [13]. Researchers are attempting to decrease the damage through ameliorate disease detection and more effective treatment like instant Trabecular Micro-Bypass (TMB). Figure 1 represents an overview of the anatomy of human eye [14]. The authors [15] gave a brief survey on state of art techniques of automatic detection of glaucoma in early stages. Critical evaluation of the methods have been conducted which include Optic cup disc ratio, Retinal Nerve Fiber Layer (RNFL) etc. These researches add value to the efficient diagnosis of glaucoma. They further summarizes the survey into 2 categories of segmentation based approaches and non-segmentation based approaches. Sarhan et al. [16] conducted the survey of current approaches to detect glaucoma that are valuable for the researchers to predict the proficiency and precision. This is an effective survey that lays the guiding details for the researcher in terms of approach of glaucoma and dataset selection for further research [16].

1.1. Major causes of glaucoma

Glaucoma is a multiplex ailment and a single test cannot give much information about the detection of glaucoma. A constant eye assessment habitually necessitates concealing for glaucoma and indicates

Table 1. List of abbreviations.

Keywords	Abbreviation	Keywords	Abbreviation
CAD	Computer-Aided Diagnosis	TMB	Trabecular Micro-Bypass
NRR	Neuro-Retinal Rim	NTG	Normal-Tension Glaucoma
OCT	Optical Coherence Tomography	KNN	K-Nearest Neighbours
IOP	Intraocular Pressure	ML	Machine Learning
CDR	Cup to Disc Ratio	AI	Artificial intelligence
RDR	Rim to Disc Ratio	SVM	Support Vector Machine
NRR	Neuro Retinal Rim	CNN	Convolutional Neural Networks
OAG	Open-Angle Glaucoma	DL	Deep Learning
ACG	Angle-Colure Glaucoma	ROI	Region of Interest
POAG	Primary Open Angle Glaucoma	OD	Optic Disk
PACG	Primary Angle Closure Glaucoma	LFDA	Local Fisher Discriminate Analysis
LTG	Low Tension Glaucoma	MMM	M-Medoids Model
ICE	Irido Corneal Endothelial Syn- drome	GMM	Gaussian Mixture Model
RAD	Relative Area Difference	OC	Optic Cup
DM	Dice metrics	ONH	Optic Nerve Head
FNN	Feed Forward Neural Network	FCNN	Fully Connected Neural Network
PNN	Probabilistic Neural Network	GT	Ground Truth

that additional inspection is needed. Glaucoma's sightlessness is inevitable, that is why initial detection is pivotal as glaucoma cure rescue endure vision but not refine eyesight [17]. Glaucoma can occur due to the enlarging of IOP, the changes in the inter-papillary, and the para-papillary area of the optic nerve head [10]. Glaucoma succession directs to few structural alterations in the region of retinal layers and optic nerve. Cup to Disc Ratio (CDR) and Rim to Disc Ratio (RDR) are numerous structural alterations that are used for glaucoma detection. Observing the values of these parameters may help in detection of glaucoma [11]. Figure 2 illustrates the fundus image of normal human eye [18]. The increase in IOP in the eye is considered as the origin of nerve optics injure. This pertains to mechanical squeezing or reduces blood passage of the optic nerve and occasionally eye pressure results in glaucoma [19]. Increased pressure changes the CDR and RDR that are considered to be the most important parameter for glaucoma diagnosis [20]. The circular zone is optic nerve concentred by the optic cup and the area

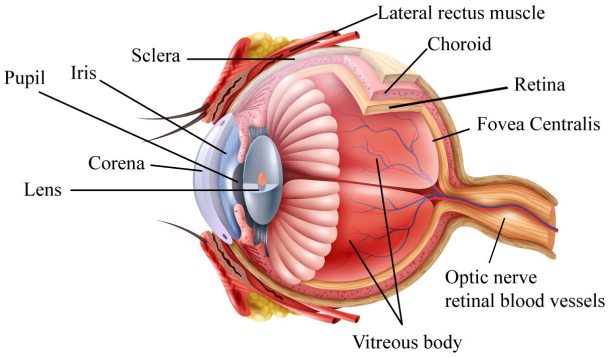

Figure 1. The anatomy of human eye [14].

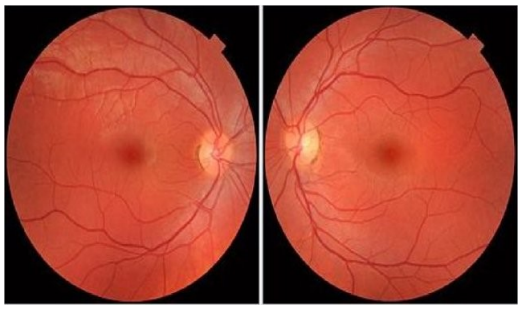

Figure 2. Fundus image of normal eye [18].

in middle is called Neuro-Retinal Rim (NRR). CDR and RDR are constructional variations consume in the detection of glaucoma [21]. In eyes with glaucoma, the growth of IOP results in the enlargement of an optic cup that causes a reduction in NRR, leading to a large CDR and a small RDR. Figure 3 illustrates a labelled fundus image [22].

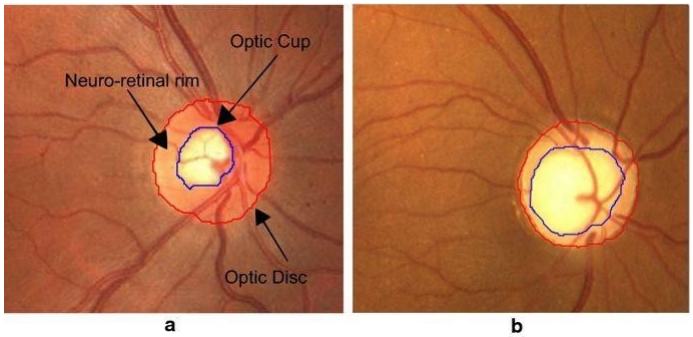

Figure 3. A labelled fundus image [22]

Patients suffering from glaucoma do not have any sort of symptoms at early stages and have no signal of illness but at the advanced stages people having glaucoma experience vision loss. Optic nerve is a blemish to work due to high pressure in eye which is affected by the high production of aqueous humor or degassing system of the liquid gets blocked. Somehow this disease is also occurred

because of genetics having this disease prior in the family. Several tests are performed with patients having suspected glaucoma like tonometry i.e. used for measuring the pressure of eyes, gonioscopy is used to check out either the angle is open or closed. Moreover, fundus imaging as well as optical coherence tomography is used for the optic nerve and the location of the retina. The thickness of retinal nerve fiber layer is diagnosed by the retinal fundus imaging, it helps in the demonstration of glaucoma. This technique is very common and used by most of the ophthalmologists. The major advantage of using this technique is that the size of retina can be measured very easily with little effort and it is portable to use.

1.2. Risks cognate with glaucoma

Since last few years, a considerable amount of studies have been conducted and results have been reported about the risks associated with glaucoma [23]. These studies stated many risk factors and their adverse effects. Figure 4 represents the risks affiliated with glaucoma. The occurrence of any

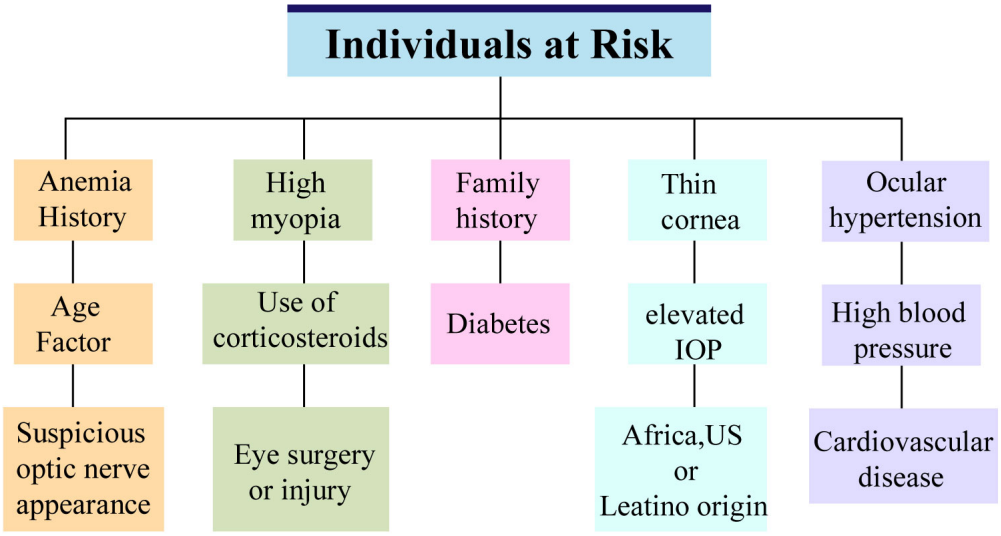

Figure 4. Risks associated with glaucoma [24].

of these symptoms in an individual does not indicate that the one is infected with glaucoma, only an ophthalmologist can determine the risk of disease onset and progression. Some of the high risk factors associated with glaucoma are (i) increased eye pressure (ii) age (iii) thin cornea (iv) hypertensive (v) diabetic patients (vi) history of injuries to eyes (vii) a family history of glaucoma (viii) nearsightedness (ix) cardiovascular diseases (x) steroid consumption (xi) rate of blood pressure (xii) severe anemia [25]. Research studies reported that 17% hypertensive, 35% diabetic and 48% individuals suffering from both diseases are at a high risk of developing Open-Angle Glaucoma (OAG). Commonly associated conditions associated to the metabolic syndrome's components comprise of hyperlipidemia (high levels of triglyceride and cholesterol), hypertension, diabetes and obesity. Research studies indicated that diabetes and hypertension increase the risk of OAG in individuals. More research efforts are being made for glaucoma treatment and to assess the impact of hyperlipidemia as glaucoma risk factor. Risk factors are important to consider since they specify a potential target for a specific treatment.

1.3. Types of glaucoma

Glaucoma is categorized into various types depending on the causes and symptoms as revealed by the researcher during the last decade. The two pre-eminent types of glaucoma are OAG further branched as Normal-Tension Glaucoma (NTG) [26] and Angle-Colure Glaucoma (ACG). Figure 5 represents the types of glaucoma. These fundamental types encompasses of 90% among all glaucoma causes [27]. The types and the causes of glaucoma are described below:

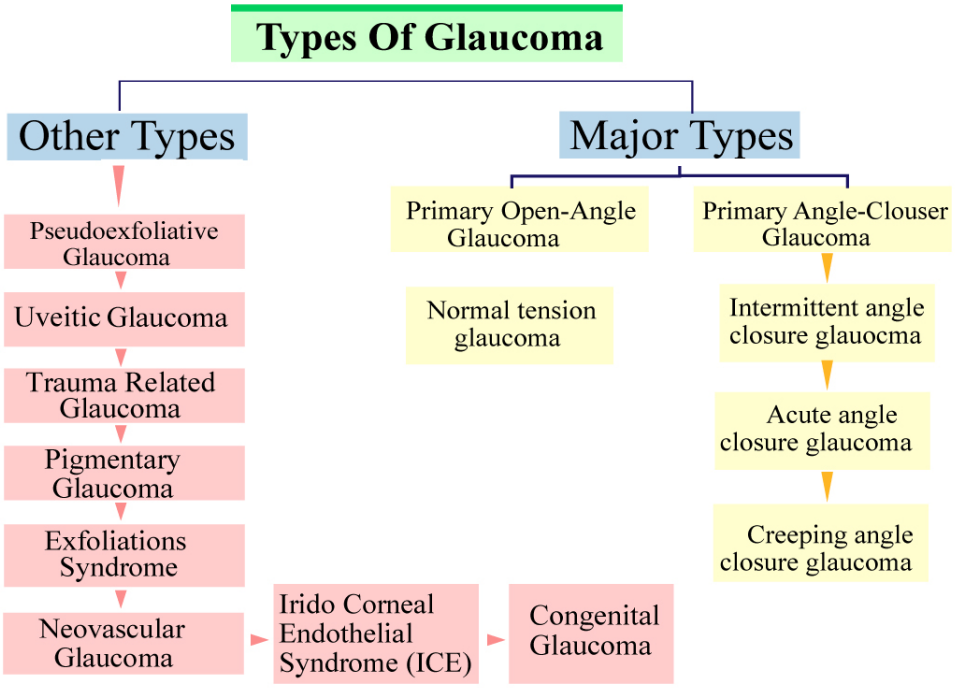

Figure 5. Types of glaucoma [26].

1. Primary Open Angle Glaucoma (POAG): Freakishness in trabecular reticulum and slow clogging of the drainage canals causes IOP to increase which in turn causes open angle glaucoma. It develops over the time and is referred to as slow poison that is lifelong lasting. Optic nerve damage and optic defect are the measuring metrics for OAG [28].

2. Primary Angle Closure Glaucoma (PACG): This is less common type of glaucoma as compared to open angle glaucoma. The causes include the damage of optic nerve and high IOP. Unlike POAG, angle closure glaucoma grows fast and needs immediate medical attention. The metrics of detection are almost similar as that of POAG i.e. optic nerve head damage, glaucomatous visual filed defect and narrow camber angle. One important measure is occludable angle used to estimate glaucoma. An occludable angle correspond to PACG if the rare trabecular meshwork is seen in less then 90° of the angle boundary [29].

3. Low Tension Glaucoma (LTG): It is also caused by the optic nerve damage but the elevation of IOP is not obligatory. Even though the IOPs of some patients are normal but still they have

normal tension glaucoma often called low tension glaucoma. People with normal IOP can suffer LTG since they may be sensitive to normal eye pressure. The main cause can be the low blood supply to optic nerve head. The metrics of detection are same as the both POAG and PACG [28]. Table 2 provides an overview of the other types of glaucoma.

Table 2. Types of glaucoma.

Types of Glaucoma	**Major Causes**
Acute glaucoma [30]	An abrupt rise in IOP due to surplus propagation of hydrous humor in hours.
Pigmentary glaucoma [31] [32]	Nearby glimpse eye has concave the same as iris have that causes hydrous humor to splatter on trabecular meshwork resulting in its closure.
Exfoliations syndrome [33]	Its color is white. Material accelerates on the lens and this causes closure to the trabecular meshwork.
Trauma-related glaucoma [34] [35]	Physical changes within an eye drainage canal because of some injuries or accidents or inflammatory conditions.
Uveitic glaucoma [36]	Ocular inflammatory disorders (uveitis) can occur for various reasons and unfortunately, glaucoma can soften up to 20% of patients. Some of these disorders tend to affect only one eye. Other forms can affect both eyes
Irido Corneal Endothelial Syndrome (ICE) [37]	The backside of cornea contains cells that scatter over the eye drainage tissue and across the surface of the iris. This leads to an increased IOP in an eye that can damage the optic nerve. These cells form accession that glue the cornea and iris and block the drainage channel system. And iris and block the drainage channel system.
Congenital glaucoma [38]	Normally babies suffer from this type of glaucoma. When a woman is pregnant than if her baby's eye drainage canal system development is not correctly building this leads to Congenital Glaucoma.
Pseudoexfoliative glaucoma [39]	Pseudoexfoliative glaucoma occurs when ash-like material peels off from the external side of the lens in the eye. This ash-like material collects within the angle between the iris and cornea and damage the whole system of the eye.
Neovascular glaucoma [40]	This type of glaucoma always related to other abnormalities, most often diabetes. Blood vessels are blocked and the eye's fluid can leave the eye's drainage canals and this will cause an increase in IOP and this kind of glaucoma is very hard to treat.

1.4. Ministrations of glaucoma

Treatment of glaucoma involves certain after-effects and financial expenses. The rudimentary treatment which is also called first-line treatment [41] is the use of eye-drops [42]. Second-line treatments encompass trabeculectomy or microsurgery [43]. Third-line treatment is given to the patients not responding to medications and are at a severe stage of glaucoma. These include laser surgery, drainage implants and other methods that help lower intraocular pressure [44]. Figure 6 demonstrates the different types of treatments associated with glaucoma.

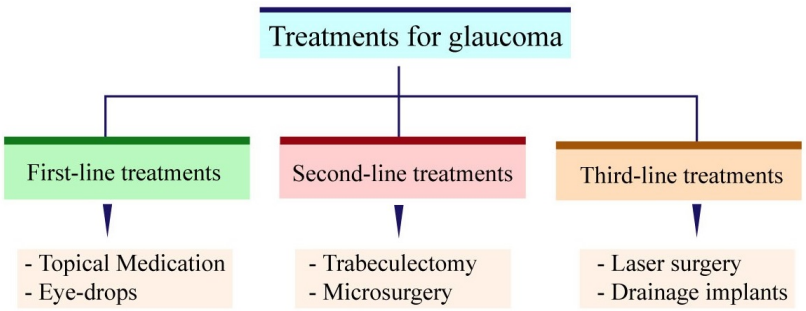

Figure 6. Treatments for glaucoma [41].

2. Approaches for the detection of glaucoma

Glaucoma is considered to be an irremediable blindness in people with an age of more than 40 years. Carrillo et al. [45] proposed a computational tool to assist automatic detection of glaucoma. The most widely applied technique for glaucoma detection is fundus imaging since it provides a trade-off between cost, size and portability. The authors reported improved results for disc segmentation as compared to the related research. Disc segmentation was done by thresholding, vessel segmentation was done by edge detection and for cup segmentation a strategy is followed that make use of vessels and cup intensities. Results obtained from a set of fundus images having percentage of glaucoma detection success was 88.5%. According to authors [45], the future work perturbs to use a larger dataset of fundus images to ensure a pro-found evaluation. Sengar et al. [46] suggested a method for the detection of suspected glaucoma by practicing existence or deficiency of hemorrhages in specific area near optic disc in image having fundus features. This method is considered to be computationally efficient and provides effective and accurate results on the diagnosis of suspected glaucoma. Salam et al. [11] proposed procedure that uses an algorithm for the detection of glaucoma having a combination of CDR and hybrid textual and different intensities features. Image organization is processed using the result that comes from both CDR as well as the classifier. According to the results [11], the proposed fusion improved sensitivity, specificity and accuracy. Poshtyar et al. [47] suggested the procedure of automatic detection of glaucoma i.e. without the aid of consultant and advance machinery. Quantitative determination is used for glaucoma detection. The method used is efficient. Khan et al. [48] proposed the techniques for detecting glaucoma in the early stage. In the proposed study [48], glaucoma is classified by CDR and NRR i.e. ISNT quadrants for the purpose of checking out that it follow or unfollow ISNT rule. Table 3 provides a description of the datasets and the reported results in term of

accuracy for the approaches that are discussed above.

Table 3. Glaucoma detection approaches.

Authors	Dataset	Accuracy
Carrillo et al. [45]	26 fundus images	88.50%
Khan et al. [48]	50 retinal images	94%
Sengar et al. [46]	140	93.57%
Poshtyar et al. [47]	300 retinal fundus images	N/A
Salam et al. [11]	50 fundus images	92%

2.1. Glaucoma detection through peripapillary atrophy

Peripapillary atrophy is said to be divided into 2 categories [49]. These categories are a-zone and b-zone. The authors states that b-zone category is associated with glaucoma progression. They further elaborate that glaucomatous eyes with PPA show faster thinning of retinal nerve then the regular eyes. In this study OCT B scan images were utilized to gain optic disc sizes. Total of 115 subjects were examined in the study. The presence of glaucoma was classified in the basis of Peripapillary atrophy. Authors argue that peripapillary atrophy is considered to be very progressive morphological diagnosis for open angular glaucoma [50]. Peripapillary atrophy is a variable that can be helpful for the detection of glaucoma. Eyes with glaucoma show large peripapillary atrophy. The technique used is confocal scanning laser tomography and automated static threshold perimetry for measurement of peripapillary atrophy [51]. The test was carried out on 102 eyes samples. Here the entropy was divided into 2 zones. First zone was central zone with visible and large vessel and second zone called peripheral with hyper pigmentation. The authors concluded that the peripapillary atrophy is associated with optic nerve damage which is the major cause of glaucoma [51].

2.2. Glaucoma detection through Retinal Nerve fiber

Here researchers used retinal nerve fiber layer RNFL , optic nerve head and muscular thickness parameters to classify healthy and effected eyes [52]. The total eyes under examination were 80. Stratus OCT was used for the scanning of the patients. Authors state that RFNL parameter has higher AUC then other parameters under consideration [52]. Authors tested 64 patients either with healthy eyes or glaucomatous eyes [53]. Each patient went through five oct scans. Linear regression slopes of the patients were measured with glaucoma and non-glaucomatous eyes. Kaplan-Meier survival curve analysis was done for the patients and a significant progression rate was recorded [53].

2.3. Glaucoma detection through Vessel displacement

The authors describe the relationship between cup width , cup depth and vessel displacement. The sample on which the study was conducted consisted of 826 eyes [54]. Fixed image separation method was used to obtain the colored graphs. The vessel displacement was estimated on a scale from 0 to 4 positive numbers. Finally they conclude that the depth of the cup and the vessel displacement are very much correlated [54]. The authors studied 16 eyes of minipig. using fundoscopic photography and fluorescein angiography [55]. The change in glaucomatous eyes was studied. These changes

were compared with the previous results. The results found in human and minipig were different and interesting. Angiography changes in minipig were negligible as compared with human eyes diagnosed glaucoma. The eyes with glaucoma of minipig showed no changes. However in the eyes of human with open angle glaucoma both the arterioles and the venues are displaced [55]. The automation of glaucoma has been an important research area for the researcher for the last two decades. Segmentation approaches discussed above are being widely used for the detection of glaucoma due to their improved results. The segmentation approaches have the advantage of being cost effective and providing accurate result hence the trade-off between size, cost and portability are achieved. Image segmentation is done by selecting appropriate feature that needs to be examined however, how to select the suitable image feature and classifier is the challenging issue that are faced by the researchers using segmentation approaches [56]. Pattern based approaches are very helpful for the detection of glaucoma. Since ONH have the structural characteristics which are well understood and verified in several studies and medical institutions [57] [58]. Since the parameters are derived from the structural features and characteristics the results are very meaningful and efficient. These approaches are low cost, efficient and reliable [59].

In last few decades great effort has been done on automation of detection of glaucoma using different Machine Learning approaches and techniques. Machine learning deals with the large amount of data and provides the analysis of data [60]. It is a faster process in acquiring information about the data. They have a feature of learning from their mistakes and experiences. Detection of glaucoma is been achieved by using neural networks [61], SVM [62], Naive Bayes classifier, k- nearest neighbor [63], Canny edge detector [64] Fuzzy min-max neural network [65]. The main advantages of the machine learning approaches in detection of glaucoma is that they can handle large amount of datasets and can provide beneficial results. Since the machine learning approaches do not need much human interference hence the human resource is saved. The data is handled and is trained and made error free using AI. The results obtained using machine learning classifiers show significant improvement compared to the traditional segmentation approaches.

The diagram 7 illustrates the architecture called AGLAIA-MII to detect the features for glaucoma detection and pass the features to multiple kernel learning (MKL) framework which will finally make the diagnosis of Glaucoma. This is a very effective framework used by researchers for glaucoma detection.

The only disadvantage associated with ML techniques is the data acquisition, which should be good quality and unbiased. Some of the glaucoma ML detection techniques do not provide the excellent results only due to low data quality and less data sometimes. Cost and resources are some factors which are considered sometimes before using ML classifiers as they require large amount of resources and cost. This section covers the technical information about the image processing techniques, methodologies and algorithms proposed for the automatic detection of glaucoma. The researchers have done a lot of work for the diagnostics of glaucoma which resulted in number of types of approaches and algorithms. Figure 8 precisely demonstrates the commonly used computer vision techniques for glaucoma detection. In this article, we aim to present a detailed review about recent trends to detect glaucoma by highlighting the main contributions, available benchmarks for research evaluation, upcoming challenges. The limitations and drawbacks associated with the published research to detect glaucoma are discussed in detail and possible future directions are also mentioned. We aim to discuss the glaucoma detection based on machine learning, simple segmentation approaches, fusion based approaches, multi-scale-based approaches, texture feature-based approaches, OCT-based approaches,

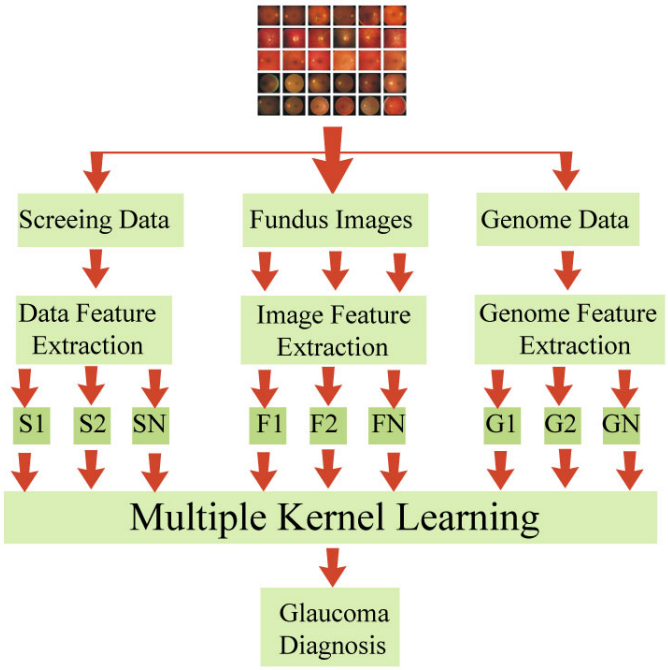

Figure 7. Working of AGLAIA-MII architecture [66].

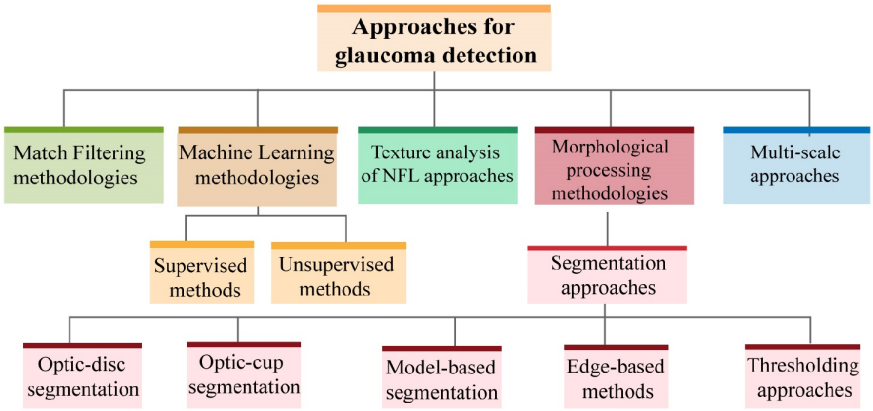

Figure 8. Classification of computer vision techniques for glaucoma detection [42].

deep-learning-based approaches, a summary about datasets/standard benchmark to evaluate glaucoma-based research is also presented, and a comparison between deep-learning and traditional approaches is also presented in this review article. The performance evaluation metrics are also presented and discussed in detail. At the end of each section, a detailed comparison is presented in the form of tables that conclude about the research methodology, datasets and performance percentage for each of the selected research model.

3. Machine Learning approaches for glaucoma detection

Machine learning is an entreaty of artificial intelligence that has been given great attention. This provides the system with the ability to learn and improve the by the experience and in turn enhance the efficiency of the output without telling it what to do by programming. Since last two decades, ML approaches are used for the detection of glaucoma [67]. Dey at el. [68] in the year 2016 proposed ML approach for automatic glaucoma detection using SVM as a classifier. In this approach [68], the authors applied to pre-processing on the image which improved the contrast of the images and removed the noise. The authors observed that the pre-processing has a major impact on the overall efficiency of the method. They took 100 images for tanning while using SVM as classifier. After pre-processing, image normalization and color conversion were performed. Afterward, feature extraction was done using the principal component analysis method. Finally, SVM was applied which had the training and testing data to classify the images as glaucomatous or non-glaucomatous. In this approach, the final results were stated as follows SVM classifier has accuracy rate 96%, sensitivity 100%, specificity 92%, positive predictive accuracy 92.59% and negative predictive accuracy 100%. Silve at el. [69] proposed the use of a hybrid feature set made up of texture and structural features of retinal image for accurate glaucoma detection. Optical Coherence Tomography (OCT) was used for early-stage detection of glaucoma and ML approaches were used for automated glaucoma detection whereas KNN shows its 90% accuracy in results.

Akram et al. [70] presented an approach that relies on the extraction of features from the OD region. Both spatial and spectral features were extracted to construct the multivariate model and LFDA is used to conduct a supervised intensification of features. The recognition of m-medoids is a cluster of data, another component that was added to analysis was ROI. The authors erect multifaceted with MMM to codify glaucoma. The proposed approach was compared to other classifiers such as SVM, GMM, KNN, and Multilayered Perceptron's. On average, their approach attained 91.7% accuracy, a positive predictive value of 78%, 92.7% specificity and a sensitivity of 84.6. Moreover, GMM is another classifier that achieved almost similar results as LFDA with a Gaussian distribution of 620. The main focus of the study is to enhance the performance of classification by integrating feature enhancement through supervised learning using LFDA.

Acharya et al. [5] presented an approach to extract features of the whole image for glaucoma classification. In the first step, images were converted to gray-scale via adaptive histogram equalization. Thereafter, to obtain textons, a total of four filter banks were utilized respectively. Then, features were extracted via local configuration pattern and this was to be done by using previously extracted textons. Authors used four filters and after extraction of results from all of them authors decided one between them. The authors obtained a total of 17808 features. Therefore, the authors wants to reduce this number so they decided to apply a new method. By applying a sequential floating forward search they decided to select the set of features. Afterwards authors applied student t-test to rank the selected features and choose those features that have a p-value of ¡ 0.05. They used total of Five classifiers, namely discriminate classifier, KNN, decision tree, probabilistic neural network and SVM with 10-fold cross-validation applied. The proposed approach resulted in 95.7% accuracy, a sensitivity of 96.2% and a specificity of 93.7%.

In this paper [71], choose mass screening because it would diagnosis glaucoma in early stages in the vast population. An automated diagnosis technique is required for mass screening. Authors proposed

an automation that is consists of optimal wavelet transformation ,preprocessing, ,classification modules and feature extraction. From fundus images statistical features are extracted via hyper analytic wavelet transformation (HWT). As phase information is preserves by the HWT and is appropriate for feature extraction. Features are classified via SVM with the help of a Radial Basis Function (RBF) kernel. To avoid premature convergence area screening and Group Search Optimizer (GSO) are embedded in Particle Swarm Optimization (PSO) framework. hybrid algorithm increased the fitness by 9.4% and 6.1%, in the test runs as Compare to conventional PSO. This success rate is achieved with the help of search ability of PSO. Furthermore, algorithm also maintains PSO population's identity.
In this paper [72], the authors discussed the automatic identification of glaucoma and normal classes with the help of Discrete Wavelet Transform (DWT) and Higher Order Spectra (HOS) features. Then features are given to the SVM classifier either in linear or polynomial order that is 1, 2, 3 and Radial Basis Function (RBF) to select the best kernel function for the selection of automated decision making. to identify the normal and glaucoma images automatically. Authors use Support Vector Machine classifier with the kernel having polynomial order 2 and achieve an accuracy of 95%, sensitivity and specificity of 93.33% and 96.67% respectively. In this paper [73], the authors used automatic screening of Glaucoma from fundal retinal images in a person via complex wavelet features and trispectrum. At first, gray-scale conversion is done and then Random transform and histogram equalization is done to enhance the input retinal image. optic disk segmentation is carried out using region separation and binary conversion. After that features are extracted with the compensation of trispectrum, complex wavelet and segmented area features. For the classification of the images to check whether it's normal or glaucoma training of neural network will be processed via conjugate gradient descent algorithm. Rim-One database is used in this experiment. comparison was also made in this paper with the exiting methods and Proposed technique has outperformed existing method by having better accuracy value of 81%.

3.1. Fundus image applications of ML

Lim et al. [74] implemented the deep learning approach on OD segmentation. This technique allows to obtain correctness of OD segmentation and that is used to govern the most biding situations for manual examination. Maninis et al. [75] inspected fundus images to segment OD and blood vessels respectively. Al-Bander et al. [76] segmented both fovea and OD and used the technique based on deep learning approach with an accuracy of 97.5%. Mitra et al. [77] recently reported some drawbacks of Al-Bander et al. [76] work while arguing that he uses gray-scale images data loss occurs. To avoid these drawbacks like in [75] [76] of OD segmentation, the authors used batch-normalization in CNN. Mitra at el. [77] took fundus images to detect glaucomatous OD. This technique used a trained model with dataset i-e ImageNet and its output is replaced by the new layer for output 2 nodes for glaucoma and normal classes respectively. When this work was compared with the pervious work we found out that this work gathers a large amount of data and is considered the most robust one compared to the rest of the works.

FCNN [78] is a very famous and re-known technique for classification-based problems associated with biomedical images [79]. X Sun et al. [80] make use of much faster RCNN architecture for OD segmentation from fundus images that are based on deep object detection architecture respectively. Figure 9 below shows the flow of basic neural network and how it works.
Ghassabi et al. [81] integrated approach of cup segmentation and ONH using SOM i-e self-organizing

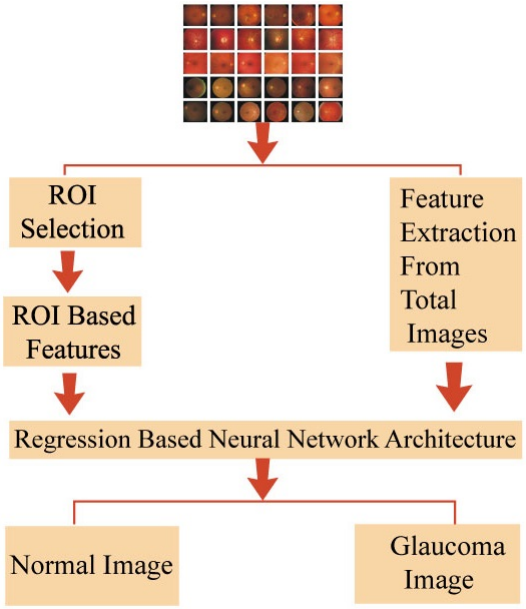

Figure 9. Basic neural network architecture.

maps for the assessment of glaucoma.it was an effective approach when there were unclear NRR, low intensities of OC, and non-obvious para-papillary shrivel. Table 4 represents a summary about various techniques that are discussed above.

4. Simple segmentation approaches

In this section different segmentation approaches will be discussed i.e. optic disc segmentation approaches, optic cup segmentation approaches, and a combination of optic disc and optic cup segmentation. While in most of the published research, optic disc segmentation approaches are described and in others, only optic cup segmentation approaches are used while some other published research models have only concerned with a mixture of the optic cup and optic disc segmentation approaches. But here we have focused on the optic disc, optic cup and their mixture of approaches.

4.1. Optic disc segmentation approaches

According to Cheng et al. [84], segmentation of disc is very crucial in the detection of different applications concerned with computer-aided systems, including detection of glaucoma using fundus images. Ahmad et al. [85] stated that the segmentation mainly depends on searching disc pixels that are mostly centered. It has been specially studied for the It has been extensively studied for solicitation in the diabetic shielding procedure in Kavitha et al. [86]. Zhang et al. [87] stated the problems related to segmentation and the disc is track down. According to experimental results, the proposed research outperformed the state-of-the-art to detection of glaucoma because the segmentation techniques measures the disc boundary which is a critical task because there are several clotting between blood vessels.

Welfare et al. [88] proposed an adaptive method for the segmentation of fundus images. In this re-

Table 4. Summary of glaucoma detection approaches based on ML techniques.

Authors	Methodology	Datasets	Accuracy
Ghassabi et al. [81]	SOM NN	SEED-DE, DRIVE,RIM-ONE	97.50%
Lim et al. [74]	3-class CNN	N/A	N/A
AL-Bander et al. [76]	CNN	MESSIDOR	96.89%
Mitra et al. [77]	CNN	EyePACS, MESSIDOR	99.05%
Maninis et al. [75]	CNN DRIU	RIM-ONE, DRIVE, DRIONS-DB,	N/A
Tan et al. [82]	CNN 7-Hiden layers	DRIVE	92.68%
Zilly et al. [83]	Ensemble Learning CNN	DRISHTI-GS, RIM-ONE	N/A
Lim et al. [74]	ResNet50-FCN	STARE, HRF, RIM, ONE, 3 CENTRE	91.60%
Raja et al. [73]	Complex wavelet features and tri-spectrum	RIM-ONE	81%

search the experiments are performed on two different sets of databases i.e. DRIVE and DIARETDB1 with a dataset of 89 images and an accuracy of 100% is achieved. Tjandrasa et al. [89] applied Hough transform at the initial level for the segmentation of optic disk. According to Tavakoli et al. [90], in retinal analysis the identification of OD or ONH are important for vessel tracking-ness and for localization of anatomical objects. In the fundus images ONH are brightest in appearance therefore localization is done with high intensity pixels with high gray scale values. Tavakoli et al. [90] presented three retinal vessel segmentation techniques for automatic ONH detection. The three databases named Mashhad University Medical Science Database (MUMS-DB), DRIVE and CHASE DB1. Although the fundus images are colored images but green channel has been used as it has clear contrast. Morphological operations have been used to increase the contrast between vessel and background as a pre-processing [90]. Image is inverted to deal with the background brightness variation in the whole fundus image so that it doesn't cause false or missed vessel detection. Multi-overlapping window has been used, its size and window overlapping have great impact on method's accuracy. For retinal vessel segmentation the edge detector used are Laplacian of Gaussian, Canny and Matched filter. Sensitivity and specificity are used as an evaluation criteria, higher values of both parameter indicates the best performance.

In an automatic diagnosis, retinal vessel detection and segmentation is a basic step and is very important subject in the field of medical image processing [91]. Although numerous methods and techniques have been proposed but none of them is fast enough to be used in real automatic detection as manual detection is very tedious process. So Bibiloni et al. [91] developed an algorithm for real-time retinal segmentation based on fuzzy morphological operations by taking into consideration the usage of cost and operations. Retinal images are being used in the detection of many medical problems such that glaucoma or diabetic retinopathy. Retinal images are acquired from fundus camera. These images

are very noisy, blurred and low contrast so there is uncertainty which can cause lack of information and indefinite. To enhance contrast authors used top-hat transformation and by taking the advantage from fuzzy logic and set theory in fuzzy mathematical morphology has been used to handle it the uncertainty present in the images. The DRIVE and STARE databases has been used and precision, accuracy, specificity and sensitivity are used as a performance evaluation criteria. The results have been evaluated and compared with other methods of state-of-the-art. According to Bibiloni et al. [91] proposed method improves segmentation and has better performance when comparing with real-time systems. Agarwal et al. [92] presented an automatic techniques for strategic OD Segmentation. They used morphology-based and edge detection techniques for correctly segmentation of OD and snake-based active contour fitting has been used for exact boundary detection. For experiments 60 fundus images were used. Computational time and overlapping score have been calculated between segmented optic disc and ground truth [92]. Results shows that proposed method has more than 90% overlapping score which shows the accuracy of the method and very helpful for automatic screening of patients.
According to Pal et al. [93], the segmentation of OD in retinal fundus images is important in diagnosis process for the detection of many diseases. Pal et al. [93] presented a technique for OD segmentation based on morphological operations that has been applied on different channels of the fundus images. Contrast Limited Adaptive Histogram Equalization (CLAHE) has been performed and discussed for the choice of clip limit to enhance the contrast. RIM-ONE dataset of 290 images of glaucoma has been used. To make segmentation process effective by using simple canny edge detection approach various morphological techniques have been combined. The performance has been evaluated on ground truth and the parameters such as sensitivity, specificity, accuracy and overlapping ratio are used [93]. The comparison has been performed with state-of-art methods. Table 5 below summarizes all the discussed techniques for OD segmentation.

4.2. Model based segmentation approaches

Wang et al. [94] proposed model based segmentation for early detection of glaucoma. In this method the images are taken locally not globally as it works efficiently by taking a small region of the defective area. Fourier transform is used to detect the center of glaucomatous images by taking the linear operations as dimensional function of gaussian filter while the multiple features are taken as superposition of the gaussian filter Deng et al. [95]. Then features are separated by K-Means clustering technique. Different models are selected based upon the size of the block which varies and it depends on the researcher criteria. The akakie information criteria is used to select the best model over the rest. The dataset used here is 20 and it is obtained by STARE dataset. The image is first converted in to gray scale. The model used is cheap and easy to use but it has some difficulty as it is quite robust in its functioning and probably uncertainty occur due to low scale ratio. The algorithm works best with the specificity of 93% and having a sensitivity factor of 82%.

According to Vermeer et al. [96] there are so many methods that are used for the early detection of glaucoma in fundus images but the result are not always accurate and satisfactory but he present a unique model for this purpose. The approach used here is the Laplace. The image used in this model are selected by Gx, a laser based device and it selected two kinds of images. The blood vessels obtained by this method are of both types i.e. light as well as dark. A gaussian filter is applied here to smoothen the corresponding image. This model first find out the dark portion and then comes to the inner portion. Laplacian filter is applied and objects are divided by thresholding one to one, two or more objects.

Table 5. Summary of segmentation-based approaches.

Authors	Methodology	Datasets	Accuracy
Cheng et al. [84]	Superpixel classification	650	N/A
Ahmed et al. [85]	Thresholding, edge-based	121	97.50%
Kavitha et al. [86]	Automatic segmentation	36	N/A
Zhang et al. [87]	ARGALI approach	1564	96%
Welfer et al. [88]	Adaptive morphological approach	89	100%
Tjandrasa et al. [89]	Hough transform	30	75.56%
Tavakoli et al. [90]	Automatic OND detection based on segmentation based approaches and mathematical morphology	MUMS-DB,DRIVE and CHASE DB1	N/A
Bibiloni et al. [91]	Fuzzy morphological algorithm for real-time system	DRIVE and STARE	93.8% for DRIVE. 95.4% for STARE.
Agarwal et al. [92]	Morphological techniques and active contour fitting	60 fundus images	N/A
Pal et al. [93]	Mathematical morphology for OD Segmentation	RIM-ONE database of 290 fundus images	98%

Noise is removed by separating small objects but this process will remove fine details of important features, so to sort out this problem fragment vessels and then perform separation. Orlando et al. [97] proposed a conditional random field model for the diagnosis of glaucoma. The different parameters are used here and are learned automatically by the help of vector machine. Different datasets are used for this purpose. The summary of the model-based approaches is shown in Table 6.

4.3. Optic cup segmentation approaches

Segmentation in the optic cup is more difficult than the segmentation of optic disk because the density of blood vessels is high in the optic cup compared to the optic disk. Moreover, the gradual change of intensity in the optic cup and NRR make the segmentation more difficult in optic cup. When

Table 6. Summary of model-based approaches.

Authors	Methodology	Dataset	Accuracy
Wang at el. [94]	Vessel segmentation algorithm	STARE	93%
Deng at el. [95]	Adaptive Gaussian filtering algorithm	Private dataset	N/A
Vermeer et al. [96]	Laplace and thresholding segmentation	GX images	Sensitivity 92% and specificity 91%
Orlando et al. [97]	Potts model	DRIVE, STARE, CHASEDB1, and HRF.	N/A

a person has glaucoma then due to its presence cup size automatically changes. According to Ingle et al. [98], the detection of glaucoma CDR is a crucial method having a region of the cup to disc. In this proposed methodology region of the cup is detected from the dataset. ROI varies differently in different images. An automatic cup region procedure has been used here in this research [98].

Joshi et al. [99] proposed an automatic technique for early detection of glaucoma. In this research, an automatic OD parametrization technique is applied to segment monocular retinal images. Cup segmentation is done by vessel bends which are quite close to the detection of glaucoma. There exist a variation between the mathematical and photometric changes. The OC segmentation obtained in this way is quite efficient and effective. Damon et al. [100] proposed a method for automatic detection of the optic cup fused with kinks Finkelstein et al. [101] approach. Here blotches are extracted from the OD by the help of kinks and for vessel detection, the color and edges are determined with the help of patches. Xu et al. [102] proposed super-pixel-based framework by using segmentation of optic cup in glaucoma detection. Xu et al. [103] applied super pixel and different tasks are formulated with their solution using LRR approach. Table 7 concludes the above studies.

4.4. Fusion-based approaches

In computer vision and image analysis, fusion-based approaches are used to enhance the performance of image classification model [104, 105]. According to Ho et al. [106], many features are extracted for the identification and detection of glaucoma. To differentiate between optic disc and optic cup histogram, dissemination is calculated from the previous studies of optic images proposed by Chang et al. [107]. The active contour model is used for early detection using different vessels. Here for the identification of major peaks erosion and dilation techniques are used. Moreover eroded and dilated image differentiation was used for the extraction of the main peak using the reverse histogram. Wong et al. [108] proposed an automatic technique for the detection of glaucoma i.e. ARGALI and it is used for the segmentation of optic disc and optic cup. This paper makes use of SVM and NN fusion

Table 7. Summary of optic-cup segmentation approaches.

Authors	Methodology	Dataset	Accuracy
Ingle et al. [98]	Gradient method	N/A	N/A
Joshi et al. [99]	Automatic OC parameterization technique	138	N/A
Damon et al. [100]	Vessel kinking	67	N/A
Xu et al. [102]	Super-pixel framework and domain adaptive technique	482	N/A
Xu et al. [103]	Super-pixel framework Classifier learning process classification refinement scheme.	650	N/A

instead of ARGALI. Here the results show that SVM has greater consistency compared to NN which proves that SVM could be the best option in the replacement of the ARGALI approach. Figure 10 shows the architecture of SVM based technique.

Yin et al. [109] proposed a statistical model-based methodology for performing the segmentation of OD and OC. This method makes a fusion of Hough transform and optimal channels for OD segmentation. It is then enhanced to OC segmentation which is assumed to be a more critical and time taking task. Here 325 images are used for testing. The results obtained by using these approaches are promising efficient because the methods used are quite intelligent. Chandrika et al. [110] proposed K-means pixel clustering technique and gabor wavelet transform to segment images and CDR is calculated using different parameters of quantitative measures. In this research, the normal CDR ratio is 0.3 and if the CDR ratio enhances from 0.3 then it is considered to be glaucomatous otherwise it is considered to be non-glaucomatous. Annu et al. [111] proposed a Probabilistic Neural Network(PNN) for the segmentation of optic cup and optic disc. PNN classification is further divided into two different phases i.e. training and testing. The accuracy encounter here is 95% which shows the effectiveness of this approach. Fu et al. [112] proposed a deep learning approach that is M-Net which solves the problem of OD and OC segmentation together on a single system. It has several layers and these layers are responsible for the formation of the pyramid of image. Polar transformation Dhar et al. [113] also used it. The dataset used here was ORIGA.

Wong et al. [114] formulated a morphological attribute for identification of glaucoma which is termed as kinks. The different features are extracted from the images with help of edge detection approaches and the different edges of the vessels provide kinks and consequently with the help of these kinks the cup and disc surroundings are measured. The results show that these kinks provide very little error in measurement which proves that these methods are quite beneficial to use. Figure 12 illustrates the basic deep learning architecture that is being used for the detection. Murthi et al. [115] proposed an automatic approach for the extraction of features from colored images. For the detection of glaucoma, CDR is a core feature that should be calculated very carefully. An algorithm is proposed here which is used to enhance the accuracy of the boundary and is known as least square fitting. ARGALI method is used for the segmentation of optic disc and optic cup together. This algorithm improves the clinical

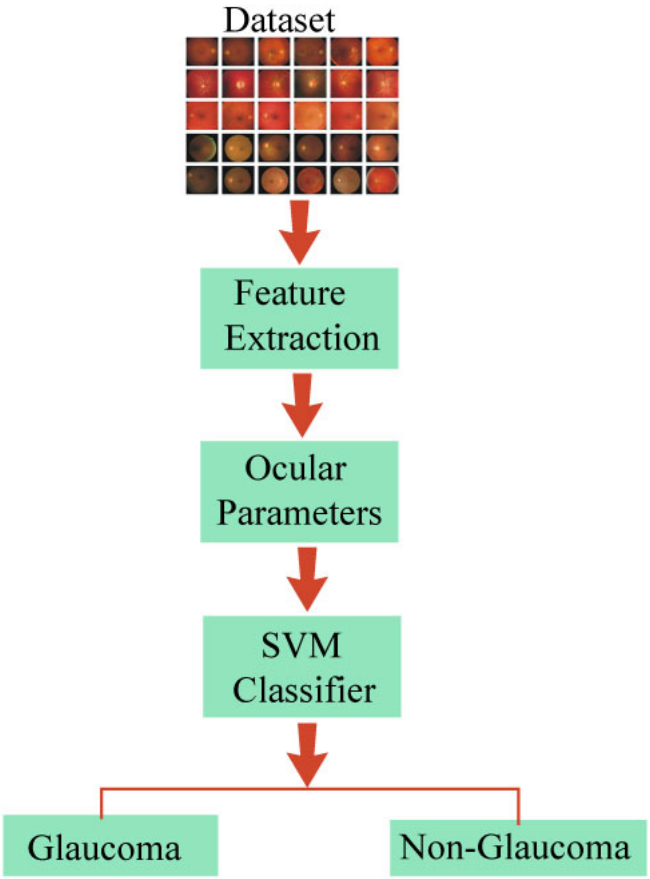

Figure 10. Simple SVM based technique architecture.

elucidation of glaucoma and all implementation is done in MATLAB. According to Khalid et al. [116], CDR or measurement is important for the detection of glaucoma in fundus images and due to the ambiguous color pattern between the optical cup and the disk and its calculation is difficult. Khalid et al. [116] proposed Fuzzy c-Mean(FCM) techniques for the segmentation of optic cup and disc with aim to measure CDR. From the RGB fundus images the green channel has been used as green channel has better contrast than others. Basic morphological operations such as erosion and dilation are used to reduce vernacular. The elimination of vernacular part plays vital role to get effective segmented results and the values of accuracy, sensitivity and specificity are improved. Ground truth and ROC analysis have been used as an evaluation of proposed method for segmentation [116]. The result shows the effectiveness of FCM segmentation algorithm with morphology.

According to Nugroho et al. [117], the retinal abnormality such as glaucoma is diagnosed by measuring the CDR (cup-to-disc ratio) so segmentation of both optic cup and disc is important. Two approaches for segmentation of fundus images are proposed by Nugroho et al. [117]. For optic disc segmentation active contour with integration of reconstruction of morphology has been used and for optic cup segmentation reconstruction of morphology with convex hull has been utilized [117]. In segmentation process retinal vessel removal for cup segmentation and channel extraction with some

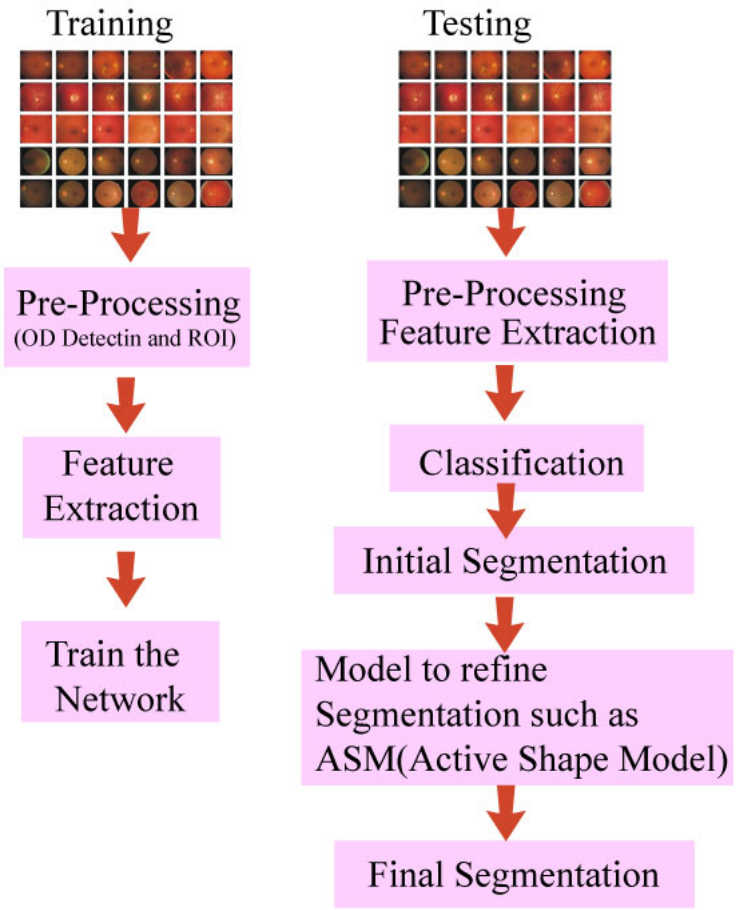

Figure 11. Flow of deep learning architecture.

contrast improvement to reduce noise for optic disc segmentation has been performed. The experiments have been performed on 50 colored images of DRISHTI-GS dataset. The parameters such as accuracy, sensitivity and specificity are used to evaluate the performance of the proposed approach [117]. Table 8 summarizes the methodology, datasets and the metrics that are used for the evaluation of the research models that are discussed here.

5. Multi-scale based approaches

Zhang et al. [118], presented a segmentation algorithm for recognition of vessel or non-vessel pixels based on a texton dictionary. In contrast to the previous researches that learned filter parameters from image pixels that were labeled manually, the proposed approach derived filter parameters from a small collection of image features termed as keypoints. Gabor Filter bank was used for the extrication of keypoints that represented features based on a SIFT inspired approach. The keypoints were determined from the validation set, the seeds derived from the validation set are used to initialize k-means clustering technique which is ultimately used to create a texton dictionary for some other training set. Testing is performed using NN classifier and DRIVE database is used for evaluation. The experiments

Table 8. Summary of fusion based approaches.

Authors	Methodology	Dataset	Accuracy
Ho et al. [106]	Active contour model	N/A	N/A
Wong et al. [108]	ARGALI SVM	N/A	N/A
Yin et al. [109]	Statistical model-based segmentation	325	N/A
Chandrika et al. [110]	K-Means pixel clustering technique, Gabor wavelet transform	N/A	N/A
Annu et al. [111]	PNN	20	95%
Fu et al. [112]	M-Net	650	N/A
Wong et al. [114]	Kinks	27	N/A
Murthi et al. [115]	ARGALI	N/A	N/A
Khalid et al. [116]	FCM with morphology	27 HRF images	90.26% for OC and 93.70% for OD
Nugroho et al. [117]	Morphological reconstruction-based segmentation for OC and OD	50 colored images of DRISHTI-GS.	99.13% for OC. 96.30% for OD.

demonstrated that the robustness of extracted clusters based on kerpoints as compared to the manually labelled pixels. The textons mitigate the problems associated with inter and intra-observer variability and appeared to be a better representative of vessel/non-vessel classes. According to Li et al. [119], ground truth is critical for evaluation of segmentation algorithms, however, the ground truth estimation from manual segmentation collections remains a challenging task. To deal with inter-rater variation there is a need to create a proper estimation approach. The authors performed an analysis in order to develop a better understanding and investigate the significance of patterns collected from manual segmentation on ground truth. The authors proposed an approach based on level-set to estimate ground truth using a probabilistic formulation. Segmentation is considered to be the first step according to the authors for computer-based applications and its accuracy is also very important. Computer-based skin lesion procedures that are used for the segmentation also become crucial. Preceding design information is used in the model. Experiments were done on both artificial as well as natural data and it is proved that preceding information gives more close, original and accurate results toward GT.

Ricci et al. [119] introduced vessel segmentation for the diagnosis of the retinal diseases that are computer-aided i.e. glaucoma. Here a line detector is applied on the green channel from RGP of the retinal image. The purpose of using the green channel is it provides the best result towards vessel

background. The vessels have a shiny texture compared to backcloth. Moreover, the vessels seem blazing over the green channel so it is preferred here to use a green channel. Two different segmentation procedures are also used here. Both the segmentation procedures give efficient results. Fraz et al. [120] proposed a supervised algorithm for segmentation of retinal images. A supervised algorithm is used for the instinctive process of segmentation. Two databases that are DRIVE Niemeijer et al. [121] and STRIVE Choi et al. [122] are used for image manipulation as well as the segmentation of retinal fundus images. The algorithm has a training image at the start, then vessel features are extracted from the training image and samples are labeled. The labeled samples have manual segmentation initially then these labeled samples are trained with the help of the classifier. Then test images are taken and again vessels are extracted the same as extracted for the training images. Then vessel features and classifiers together perform vessel classification and finally the image is segmented. The average accuracy achieved is 95.79%.

According to Zhang et al. [123], vessel segmentation problems in the retinal fundus images are considered to be a very challenging and critical scenario. Here machine learning paradigm is proposed for the identification of the texture features of the retinal images that are termed as texons. This paper also proposed a filter bank that is used for the extraction of features, edges and different changes that occur in an image. DRIVE and STARE databases are used and give efficient results when 20 images are encounter here. Table 9 summarizes the methodology, datasets and the metrics used to evaluate the research discussed.

Table 9. Summary of multi-scale approaches.

Authors	Methodology	Database	Accuracy
Zhang et al. [118]	Retinal vessel segmentation using multi-scale texton.	DRIVE	95.05%
Li et al. [119]	Manual segmentation, GT algorithm	XOR STAPLE	N/A
Ricci et al. [119]	Retinal vessel segmentation	DRIVE	94.52%
Fraz et al. [120]	Gaussian mixture model	DRIVE STARE	95.79%
Zhang et al. [123]	Machine learning paradigm	DRIVE	95.91%

6. Texture feature-based approaches

According to Septiarini et al. [124], the area of RNFL has textured surface with a number of streaks or ridges of white color and their texture is uniformly disturbed and clear in normal human eye but in the eyes of person having glaucoma the layer of nerve fiber disoriented. Septiarini et al. [124] proposed a technique based on texture attributes for automatic detection of RNFL. Co-occurrence matrix has been acquired from the outer area of optical nerve head and whether to remove blood vessels they are considered as the detection of RNFL is easy in this part. For the detection of RNFL the different classifiers are applied but Back Propagation Neural Network (BPNN) classification approach get better accuracy [124]. 40 retinal fundus images have been used in experiment and for the evaluation purpose sensitivity, specificity, and accuracy are calculated.

Kirar et al. [125] proposed a computer aided diagnosis (CAD) method for glaucoma from fundus images based on Empirical Wavelet Transform (EWT) and Discrete Wavelet Transform (DWT). After

pre-processing, the input images are decomposed by EWT , DWT , EWTDWT and DWTEWT operations and feature layers has been formed which is concatenated in next step and then normalization and selection of features has been performed. To find out best features these selected features are given in to SVD(Singular Value Decomposition) and then classification with SVM has been performed [125]. 505 images of MIAG image database has been used and many performance evaluation parameters like accuracy, sensitivity, specificity, Negative predictive rate (NPR), Rate of Negative Predictions (RNP), Matthews Correlation Coefficient (MCC) etc. are used [125]. The performance comparison of the proposed method and classification comparison with other methods has been reported. According to Nirmala et al. [126], the presence of glaucoma cause vision loss so Nirmala et al. presented wavelet-based contourlet transformation (WBCT) method for detection of glaucoma. To enhance the image contrast adaptive gamma correction technique with weighted distribution has been used. OD is segmented and blood vessels are removed by using Gabor filter. Coefficients are extracted by applying wavelet-based contourlet transformation on segmented OD region and then features are extracted from these computed coefficients. For detection of glaucoma SVM classifier is used [126]. The experiments have been performed on FAU dataset and for evaluation purpose accuracy, specificity, sensitivity and positive predictive ratio are evaluated but only accuracy has been compared with some other methods.

According to Elseid et al. [127], low contrast of RNFL in fundus images cause defects in early detection of glaucoma. Examiner may be miss the accurate detection as it relies on the experience of the inspector who is examining. So Elseid et al. [127] proposed computer aided algorithm based on RNFL texture features that accurately detects the defect in very early stage of disease. OD segmentation has been performed and then from this segmented region texture features are extracted and selected for classification purpose. For validation of the proposed algorithm RIM-ONE dataset has been used. The ROC (Receiver Operating Characteristic), accuracy, specificity and sensitivity are used as performance evaluation [127]. The reported result shows the effectiveness of the proposed algorithm that it has high accuracy. According to Claro et al. [128], the examination of glaucoma can be done in either two ways as periodic examination in which specialized instruments are necessary or it can be done via examining the fundus image through the application of digital image analysis. Claro et al. [128] presented an automatic detection approach for glaucoma. The segmentation process for optic disc has been performed fist then texture features are extracted in different color modes of image based on gray-level co-occurrence matrix and entropy [128]. Lastly, the classification by using different classifiers has been done. The DRISTHI-GS, DRIONS-DB and RIM-ONE datasets are used comparison has been performed for evaluation of the proposed method.

By taking advantage of multi-resolution wavelet transformation of localization in frequency as well as time Abdel-Hamid et al. [129] presented an approach for real time screening of glaucoma patients. The proposed method acquire textural wavelet and statistical features from the optic disc. Then selection of these feature has been performed and kNN classifier is used for classification of healthy or non-healthy fundus images [129]. GlaucomaDB and HRF datasets has been used to validate the proposed method. Specificity, sensitivity and accuracy have been computed and used as performance evaluation criteria. The reported result shows that the methods in computationally less expensive for processing of high resolution images and suitable for real time system [129]. Table 10 summarizes the methodology, datasets and the metrics used to evaluate the research discussed.

Table 10. Summary of texture feature-based approaches.

Authors	Methodology	Dataset	Accuracy
Septiarini et al. [124]	Automatic detection of RNFL with BPNN classification approach	40 retinal fundus images	94.52%
Kirar et al. [125]	EWT and DWT	MIAG/505 and MIAG/150	With MIAG/505 83.6%.With MIAG/150 88.72%.
Nirmala et al. [126]	WBCT method for detection of glaucoma	FAU dataset	89%
Elseid et al. [127]	Computer aided algorithm based on RNFL texture features	RIM-ONE	89.50%
Claro et al. [128]	OD segmentation and texture feature extraction	DRISTHI-GS, DRIONS-DB and RIM-ONE	93%
Abdel-Hamid et al. [129]	Textural wavelet and statistical features	GlaucomaDB and HRF (High-resolution fundus)	For GlaucomaDB 89.4% . For HRF 96.7%.

7. Optical coherence tomography(OCT) based approaches

Approaches based on OCT are commonly employed for the diagnosis and monitoring of glaucoma. OCT based techniques are applied by many researcher using different classifiers and great results and high accuracy is obtained [130]. Further more the incorporation of IOP measurements and visual field tests, performed along with OCT are highly related with glaucoma detection, these factors likely contributed to their higher prediction accuracy. Despite of the development and the advantage of OCT most of the clinics and physicians are not taking proper benefit of this powerful and efficient tool. The OCT scans of optic discs are widely taken and the scan of the parts that contain macula are usually missed due to which vital parts to be examined are missed [131]. Using OCT not only the existence of RNFL damage is uncovered but the pattern of RFNL damage is also analyzed. OCT scans if done properly can be used for screening [132]. The following table 11 summary for OCT-based approaches.

Table 11. Summary of OCT-based approaches.

Authors	Methododology	Dataset	Accuracy
Maetschke at el. [130]	3D CNN	OCT scan of 624 patients	94%

8. Glaucoma classification via deep learning approaches

In last few years, DL based models are used in various applications relevant to medical image analysis [133–135]. Chen at el. [134] stated that CNN are associated with DL systems that are used by the authors to discriminate between the glaucomatous and non-glaucomatous images in the proposed study. CNN net contains six layers out of which the first four are convolutional and the two are fully connected. The output of the last fully connected layer for glaucoma prediction. The authors applied the pre-processing on the image to remove the extra illuminations and get a better image. Later on, ROI is specified for the image and further computation is done on ROI. The proposed architecture of CNN consists of 6 layers through which the image is passed and final evaluation is performed. Finally, dropout and data augmentation techniques are applied to the ROI to enhance glaucoma detection accuracy. The ORIGA dataset was used which comprised of 168 glaucoma and 482 normal fundus images. The SCES dataset contains 1676 fundus images, and 46 images are glaucoma cases. The results showed that the technique provided greater results than other states of art methods applied to detect glaucoma. ORIGA dataset images were used for training and testing: 99 images were used for training and the remaining 551 images were tested.

Nguyen et al. [135] presented an unsupervised technique that is a line detector for the extraction of blood vessels. The authors focused on each pixel's position and calculate it's the corresponding gray-scale and also assigned a window over there. In the region, twelve lines were drawn down and it is noticed that all of them passing through its center. Thereafter, across each line it's average gray levels were computed. The winning line is the one with more votes and had the highest gray value amongst all and was utilized in the segmentation of blood vessels. The line detector had some draw backs i.e. it gravitate to merge close vessels. It produces an appendix at crossover points. It produces false vessel responses at background pixels near strong vessels. These drawbacks are addressed by varying the length of basic line detector. Three publicly available datasets i.e. DRIVE, STARE, and REVIEW were used for the evaluation of the proposed method. The proposed method had false positive detection i.e. 515 around the OD region. To address this problem a post-processing step can be applied to reduce the false positive and improve the performance of the method even more. Feedforward neural network (FNN): JH Tan et al. [136] Drive dataset is used with 40 glaucoma images. First of all image normalization is done before any classification that is a pre-process applied by the authors. The CNN proposed consist of 7 layers. Standard back propagation technique is used to train the data. The learning rate is set accordingly. The algorithm performs testing at the end of each training on the DRIVE dataset which achieves the accuracy of 92.68%. CNN based methods: Chen et al. [134] were the first who use a deep learning approach for glaucoma detection. He implements the CNN and CNN with dropout and CNN with 4 convolutional layers that are six-layer deep with filter size (11, 5, 3, 3) that is followed by the 2 dense layers. Chai et al. [137] dispense a structure on the

dataset of fundus images that are acquired from different hospitals by integrating both feature learned and domain knowledge from the deep learning model. Authors implied 2554 retinal fundus images from 1542 patients, out of which 1023 images are from glaucoma patients and 1531 are from people non-glaucoma patients. The authors proposed a method in which the advantage of both deep learning and domain knowledge is taken. A multi-branched neural network model is proposed to achieve the glaucoma detection. A combination of Faster RCNN, CNN and Fully convolutional network is used. Auto encoder: Pal et al. [138] prove his architecture to be more robust and given results even in low-quality images i.e. G-Eye Net architecture. Pal et al. proposed a multi- task learning procedure to detect glaucoma. Authors obtained the ROI from a colored fundus image and applies a preprocessing step using contrast limited adaptive histogram equalization. An encoder De-coder framework is applied to the data to get automated glaucoma detection i.e. G-EyeNet. This framework consists of three main parts which are 1. Encoder 2. Decoder 3. Classifier. Authors used HRF, RIM ONE v.3., DRISHTI-GS and DRIONS-DB datasets. 400 distinct images were obtained using all these datasets. The G-EyeNet showed great and significant improvement as compared to the state-of-art deep learning approaches Different glaucoma detection technique's results summary is given in Table 12.

The authors used a deep learning algorithm to detect glaucoma [139]. The algorithm named Residual Network was used and a training dataset was used. The size of dataset used was 1364 color fundus images. Image augmentation was done and a prominent increase in the accuracy was noted. The accuracy of 94.8% was calculated using the first dataset. When the same technique was applied to the second dataset the accuracy was calculated to be 99%. Hence the authors concluded that previously used DL methods can achieve higher accuracy using image augmentation. Authors introduced an automatic feature leaning based on deep learning with the usage of convolutional neural network for feature learning [140]. As traditional convolution layers use linear filter followed by non-linear filters, this convolution neural network uses more complex structures to identify the features and introduced a deep learning structures to discriminates between glaucomatous and non-glaucomatous. The datasets used by the authors are SCES and ORIGA. The authors concluded that the accuracy is much better than the state-of-art algorithms. The proposed method gives the accuracy of 89%. This method is much more efficient then the traditional methods as authors argued that the deep learning approaches gave higher results then the state-of-art approaches. Authors argue that it is difficult of compare deep learning algorithms and techniques used for glaucoma detection as many of the deep learning techniques used by different researchers use private datasets and the ones who use public datasets face the issue of overfitting as the size of datasets in many cases is small and the deep learning algorithm cannot work efficiently on small size datasets [141]. An existing model called inception-v3 was finetuned by using different methods and approaches. Data augmentation along with Contrast Limited Adaptive Histogram Equalization and normalization were applied on the dataset called RIM-ONE.Hence the results showed that problem of overfitting was addressed and now the method was more effective.

Authors proposed a deep learning approach based on convolution neural network [142]. This technique involves transfer learning and local binary pattern-based data augmentation. The CNN model used by the authors is Alex net which is responsible for transfer learning. The proposed CNN model is trained via transfer learning and the images are classified as glaucomatous and non-glaucomatous with the help of level fusion technique. They uses RIM-ONE dataset. Authors argues that the performance of the proposed method shows prominent improvement by applying LBP-based augmentation technique. Authors also adds that the approach gives promising results and these deep learning methods

helps the experts during mass screening making it automatic and very accurate. Authors give a brief overview of deep learning methods and traditional methods that are used in glaucoma detection [143]. Authors states that deep learning approaches outperformed traditional methodologies in terms of accuracy and reliability. These automatic detection techniques are also considered as support tools for the clinicians. Table 12 below summarizes the approaches.

Table 12. Summary of deep learning-based approaches.

Authors	Methodology	Dataset	Accuracy
Ragvendra et al. [144]	8-layer CNN	DRIVE	98.13%
Pal et al. [138]	Auto-encoder with CNN classifier	DRIONS-DB	N/A
Asoka et al. [145]	3-layer FNN	Private: 171	N/A
Chen et al. [134]	6-layer CNN	SCES,ORIGA	N/A
Zhixi et al. [146]	GON	private: 8000	92.00%
X Chen at el. [140]	C-CNN	SCES and ORIGA	89.0%
S Maheshwari at el. [142]	CNN transfer learning approach and LBP	RIM-ONE	93.40% for 90:10 data split 92.24% for 80:20 data split 96.0% for 70:30 data split
Nguyen et al. [135]	Line detector	DRIVE and STARE	93%
JH Tan et al. [136]	7 layer CNN	DRIVE	92.68%

9. Evaluation criteria for the glaucoma detection techniques

Automatic detection results are evaluated by using large variations of evaluation metrics. The metrics used for the evaluation must be properly defined and should co-related to the domain of the system which is under consideration. A confusion matrix as shown in Figure 12, commonly referred to as the contingency matrix or error matrix [147] is a table that gives the visual representation of the performance of an algorithm. This matrix is commonly used in the field of machine learning and classification algorithms. Figure 12 shows the confusion matrix.

9.1. Performance metrics from the confusion matrix

Some of the terms used in the confusion matrix need a little explanation for the better understanding of the evaluation [67]. Some important terms are described below and their formulas are given in Table

Confusion Matrix		Target			
		Positive	Negative		
Model	Positive	a	b	Positive predictive value	a/(a+b)
	Negative	c	d	Negative predictive Value	d/(c+d)
		Sensitivity	Specificity	Accuracy = (a+d)/(a+b+c+d)	
		a/(a+c)	d/(b+d)		

Figure 12. Confusion matrix.

13.

1. Accuracy: is termed as the percentage of the correct predictions made.
2. Precision: also termed as Positive Predictive Value and determines the percentage of correctly classified positive instances.
3. Negative Predictive Value: gives the percentage of correctly classified negative instances.
4. Recall: also referred as sensitivity, gives the percentage of actual positive instances identified correctly.
5. Specificity: the percentage of actual negative instances identified correctly.
6. True positive TrP: refers to correct prediction of event values.
7. False-positive FlP: determines incorrect prediction of event values.
8. True negative TrN: is used for correct prediction of no-event values.
9. False-negative FlN: gives incorrect prediction of no-event values.

Table 13. Overview of evaluation metrics.

Metric	Formula
Accuracy	(TrP + TrN)/(TrN + TrP + FlN + FlP)
Recall	(TrP)/(FlN + TrP)
False-positive rate	(FlP)/(TrN + FlP)
Specificity	(TrN)/(TrN + FlP) or 1 minus False-Positive Rate
Precision	(TrP)/(FlP + TrP)
Prevalence	(FlN + TrP)/(TrN + TrP + FlN + FlP)
F-measure	(2 x Precision xRecall)/(Precision + Recall)
Optic disc overlap	TrP/TrP+FlN+FlP
CDR error	CDR(GR)-CDR(PRP)
ISNT rule	OD - OC (Obtain the thickness in all 4 quadrants)
Relative area difference (RAD)	FlP+FlN/GT
Dice metrics (DM)	2*TrP/FlP+TrP+FlN

9.2. Datasets available for retinal images

Most of the techniques that are discussed in this survey use the publicly available datasets. These datasets are mentioned in the table below which gives a brief description and understanding of the datasets. These are the datasets which are commonly used by the researches to carry out the proposed approaches and conclude the findings. Table 14 summarizes the datasets that are available and can be used for glaucoma detection research.

Table 14. Datasets available for automatic glaucoma detection.

Dataset Name	Description
Drishti-GS [148] [149]	This dataset is partitioned into training and test image sets respectively. The training set comprise of 50 images, with ground truth providing information regarding region boundary, segmentation soft map and Cup-to-Disk ratio for each image. Whereas the testing set contains 51 images and the ground truth for test set is available only upon registration.Image size and resolution is 2896×1944 pixels and PNG uncompressed image format is used. The retinal image type of the dataset is Fundus Images .
HRF Dataset [150].	HRF is publically available database consisting of high-resolution fundus images. The dataset is composed of three sets of fundus images: comprising of the healthy retinas, glaucomatous and DR retinas. In the first set, 15 images of healthy patients are included which do not contain any instance of retinal pathology. The next set is comprised of 15 retinal images of patients with DR exhibiting pathological changes, such as bright lesions, neovascular nets, spots after laser treatment and hemorrhages. The last set includes 15 images of patients with advanced stage glaucoma and showing symptoms of focal and diffuse nerve fiber layer loss. The retail type of the dataset is Fundus images. The image quality of the database is 3304 x 2336 pixels.
ONSHD [151].	There are 99 fundus images taken from 50 patients.The dataset type is Fundus images. Images were captured using Kowa VX-10 alpha digital fundus camera with 50 degree field of view (FOV). The images have resolution of 4288x2848 pixels and are stored in jpg file format. The size of each image is about 800 KB.
IDRiD [152].	IDRiD is a recently introduced retinal fundus image database publicly available and consists of 516 images organized in two categoeies: 1.Retinal images that exhibit symptoms of DME and/or DR 2. Normal retinal images without any indications of DME and/or DR.
RIGA dataset [153].	The RIGA dataset comprises of 750 images collected from three sources and 4500 manual marked images. The images are saved in JPG and TIFF format and contain both glaucomatous and normal images.The resolution of 3 sources are a. MESSIDOR 2240x1488 PIXELS (460 Images) B. Magrabi eye center Riyadh 2743x1936 (95 Images) c. Bin Rushed Ophthalmic center in Riyhad 2376x1584 (195 images) The retinal image type of the dataset is Fundus images

DRIONS [154].	It comprises of 110 retinal images with image resolution of 600×400 pixels and the optic Disc annotated by two experts with 36 landmarks.The resolution of the dataset is 600x400. The retinal image type is Fundus images .
DIARETDB1 [155].	It consists of 89 colored fundus images with a sample of 5 normal and 84 images exhibiting mild non-proliferative symptoms of diabetic retinopathy.
ORIGA [156].	Consist of 650 images. 168 glaucomatous and 482 non glaucomatous.
ACRIMA [157].	The dataset is avaiable publicly, consisting of 705 labeled images, 396 of which are glaucomatous and 309 normal images.
ACHIKO-I [158].	179 images split into two subsets to serve different purposes. OD Segmentation, OC Segmentation, repeatability study and cross modality study.
ACHIKO-K [159].	It consists of 258 images annotated manually alonwith their clinical diagnosis details. The images in ACHIKO-K are collected from patients suffering from glaucoma and contain rich information related to glaucoma pathological symptoms , e.g. optic nerve drusen, hemorrhage and optic cup notching, etc. Multiple images are taken from patients suffering from glaucoma having age between 27 to 85 years during 2008 to 2012 time span. A total of 258 fundus images are available in database, where 144 are from glaucoma tic eyes and 114 are captured from normal eyes.
RIM-ONE [160].	The database consists of 169 ONH images collected from 169 full fundus images of different individuals.
SCES [161].	There are 1676 images in this dataset.
ONHSD [162].	This dataset comprises of 100 retinal fundus images.
AGLAIA-MII [66].	The dataset consists of 2258 individuals with genome data, image data and clean screening data. Among the 2258 subjects, 100 were diagnosed to have glaucoma and the rest were normal.
SERI [163].	There are 104 fundus images available in this dataset.

10. Deep learning approaches vs traditional approaches

A brief comparison has been conducted among the approaches with deep learning methodologies and traditional methodologies. Mostly the results of DL approaches seem to have high accuracy and performance. In the domain of image processing and method automation DL has pushed the limits and have given extra ordinary results. ML exhibited high sensitivity and specificity for the detection of glaucoma and hence traditional approaches are considered less effective than the former one. DL is largely based on Artificial Neural networks which is a brain like structure and works according to how brain does. Since the trained neural networks are used and are not programmed hence they give greater accuracy than the traditional approaches. Table 15 summarizes the study and shows the quantitative results.

Table 15. Summary of deep learning approaches vs traditional detection approaches.

Techniques	Authors	method	Dataset	SP	Accuracy	AUI
Lesion detection	Haloi et al. [164]	5-layer CNN	Messidor	96%	97%	N/A
Lesion detection	Antal et al. [165]	Ensemble model	Messidor	90%	90%	91%
Cup-to-Disc-Ratio and GON detection	Jagadish Nayak et al. [166]	Morphological techniques and neural network classifier detecting	Dataset	90%	100%	80%
Cup-to-Disc-Ratio and GON detection	Zhixi Li MD et al. [146]	Glaucomatous optic neuropathy based on color fundus photographs: deep	N/A	95.60%	92.00%	99%
Retinal vessel segmentation	Leopold et al.	FCN using RETSEG13	DRIVE	94.78%	N/A	N/A
Retinal vessel segmentation	Staal et al. [167]	Knn classifier	DRIVE	94.22	N/A	N/A
AMD classification	Kankanahalli et al. [168]	N/A	SURF	91.80%	91.30%	92.30%
Diagnosis of Glaucomatous Optic Neuropathy	Mohammad Norouzifard et al.	CNN and multilayer NN	RIMONE public dataset	98.16%	N/A	N/A
Diagnosis of Glaucomatous Optic Neuropathy	Krishna prasad et al. [169]	Neural network	Drive dataset	80%	N/A	N/A

11. Conclusions and Discussion

Medical imaging systems are used to create the pictorial representation of human body to monitor various types of diseases and public health-care systems reply on these technologies. Digital image processing and computer vision techniques are used in various health-care systems to detect the diseases. Glaucoma is a type of persistent eye disorder that gradually damages the optic nerve and can lead to permanent blindness. The inappropriate intraocular pressure within the human eye is reported as the main cause of this disease and glaucoma is declared as the second leading cause to the loss of sight. The use of image analysis with CAD tools can assist the clinicians to execute the work more effectively. The main aim of this review is to present and discuss different types of research

models that can perform automated glaucoma detection. We have discussed optic disc segmentation approaches, optic cup segmentation approaches, machine learning-based approaches, fusion-based approaches, multi-scale-based approaches, texture features-based approaches and current trends about deep learning models. A comprehensive detail about the types of standard benchmarks, number of samples used in the referred research and performance evaluation criteria is discussed in detail. 1) Feature fusion based approaches have shown an effective performance than the use of one feature. 2) The hand-crafted features have shown an effective performance while using small-scale image benchmarks. 3) The experimental results show the superior performance of deep learning algorithms as compared to the hand-crafted features. 4) The computational cost and training time of deep learning-based approaches is more as compared to traditional machine learning approaches with hand-crafted features. 5) It is also observed that performance of some algorithms suffers in case when the patient is affected with multiple diseases including glaucoma. Therefore, the use of deep learning-based approaches can enhance the effectiveness of professionals when they are dealing with patients suffering from multiple eye diseases. 6) The use of deep learning algorithms with large-scale fundus image benchmarks seems to be a possible research direction in this field. 7) It is also observed that most of the researchers have used their own fundus image benchmarks for the evaluation of their research and there are few publicly available images benchmarks. Due to this reason, it is required to create a large-scale publicly available image benchmark that can be used for the evaluation of future research. This will be beneficial to identify the best performance of upcoming research evaluated on the same data-set and it can lead to development of an efficient CAD for glaucoma detection.

Conflict of interest

The authors have no conflict of interest.

References

1. A. Latif, A. Rasheed, U. Sajid, J. Ahmed, N. Ali, N. I. Ratyal, et al., Content-based image retrieval and feature extraction: a comprehensive review, *Math. Probl. Eng.*, **2019**.
2. B. Gupta, M. Tiwari, S. S. Lamba, Visibility improvement and mass segmentation of mammogram images using quantile separated histogram equalisation with local contrast enhancement, *CAAI Trans. Intell. Technol.*, **4** (2019), 73–79.
3. S. Maheshwari, V. Kanhangad, R. B. Pachori, S. V. Bhandary, U. R. Acharya, Automated glaucoma diagnosis using bit-plane slicing and local binary pattern techniques, *Comput. Biol. Med.*, **105** (2019), 72–80.
4. S. Masood, M. Sharif, M. Raza, M. Yasmin, M. Iqbal, M. Younus Javed, Glaucoma disease: A survey, *Curr. Med. Imaging*, **11** (2015), 272–283.
5. U. R. Acharya, S. Bhat, J. E. Koh, S. V. Bhandary, H. Adeli, A novel algorithm to detect glaucoma risk using texton and local configuration pattern features extracted from fundus images, *Comput. Biol. Med.*, **88** (2017), 72–83.
6. B. J. Shingleton, L. S. Gamell, M. W. O'Donoghue, S. L. Baylus, R. King, Long-term changes in intraocular pressure after clear corneal phacoemulsification: Normal patients versus glaucoma suspect and glaucoma patients, *J. Cataract. Refract. Surg.*, **25** (1999), 885–890.

7. K. F. Jamous, M. Kalloniatis, M. P. Hennessy, A. Agar, A. Hayen, B. Zangerl, Clinical model assisting with the collaborative care of glaucoma patients and suspects, *Clin. Exp. Ophthalmol.*, **43** (2015), 308–319.
8. T. Khalil, M. U. Akram, S. Khalid, S. H. Dar, N. Ali, A study to identify limitations of existing automated systems to detect glaucoma at initial and curable stage, *Int. J. Imaging Syst. Technol.*, **8** (2021).
9. H. A. Quigley, A. T. Broman, The number of people with glaucoma worldwide in 2010 and 2020, *Br. J. Ophthalmol.*, **90** (2006), 262–267.
10. C. Costagliola, R. Dell'Omo, M. R. Romano, M. Rinaldi, L. Zeppa, F. Parmeggiani, Pharmacotherapy of intraocular pressure: part i. parasympathomimetic, sympathomimetic and sympatholytics, *Expert Opin. Pharmacother.*, **10** (2009), 2663–2677.
11. A. A. Salam, M. U. Akram, K. Wazir, S. M. Anwar, M. Majid, Autonomous glaucoma detection from fundus image using cup to disc ratio and hybrid features, in *ISSPIT.)*, IEEE, 2015, 370–374.
12. R. JMJ, Leading causes of blindness worldwide, *Bull. Soc. Belge. Ophtalmol.*, **283** (2002), 19–25.
13. M. K. Dutta, A. K. Mourya, A. Singh, M. Parthasarathi, R. Burget, K. Riha, Glaucoma detection by segmenting the super pixels from fundus colour retinal images, in *2014 International Conference on Medical Imaging, m-Health and Emerging Communication Systems (MedCom.)*, IEEE, 2014, 86–90.
14. C. E. Willoughby, D. Ponzin, S. Ferrari, A. Lobo, K. Landau, Y. Omidi, Anatomy and physiology of the human eye: effects of mucopolysaccharidoses disease on structure and function–a review, *Clin. Exp. Ophthalmol.*, **38** (2010), 2–11.
15. M. S. Haleem, L. Han, J. Van Hemert, B. Li, Automatic extraction of retinal features from colour retinal images for glaucoma diagnosis: a review, *Comput. Med. Imaging Graph.*, **37** (2013), 581–596.
16. A. Sarhan, J. Rokne, R. Alhajj, Glaucoma detection using image processing techniques: A literature review, *Comput. Med. Imaging Graph.*, **78** (2019), 101657.
17. H. A. Quigley, Neuronal death in glaucoma, *Prog. Retin. Eye Res.*, **18** (1999), 39–57.
18. N. Salamat, M. M. S. Missen, A. Rashid, Diabetic retinopathy techniques in retinal images: A review, *Artif. Intell. Med.*, **97** (2019), 168–188.
19. F. Bokhari, T. Syedia, M. Sharif, M. Yasmin, S. L. Fernandes, Fundus image segmentation and feature extraction for the detection of glaucoma: A new approach, *Curr. Med. Imaging Rev.*, **14** (2018), 77–87.
20. A. Agarwal, S. Gulia, S. Chaudhary, M. K. Dutta, R. Burget, K. Riha, Automatic glaucoma detection using adaptive threshold based technique in fundus image, in *(TSP.)*, IEEE, 2015, 416–420.
21. L. Xiong, H. Li, Y. Zheng, Automatic detection of glaucoma in retinal images, in *2014 9th IEEE Conference on Industrial Electronics and Applications*, IEEE, 2014, 1016–1019.

22. A. Diaz-Pinto, S. Morales, V. Naranjo, T. Köhler, J. M. Mossi, A. Navea, Cnns for automatic glaucoma assessment using fundus images: An extensive validation, *Biomed. Eng. Online*, **18** (2019), 29.
23. T. Kersey, C. I. Clement, P. Bloom, M. F. Cordeiro, New trends in glaucoma risk, diagnosis & management, *Indian J. Med. Res.*, **137** (2013), 659.
24. A. L. Coleman, S. Miglior, Risk factors for glaucoma onset and progression, *Surv. Ophthalmol.*, **53** (2008), S3–S10.
25. T. Saba, S. T. F. Bokhari, M. Sharif, M. Yasmin, M. Raza, Fundus image classification methods for the detection of glaucoma: A review, *Microsc. Res. Tech.*, **81** (2018), 1105–1121.
26. T. Aung, L. Ocaka, N. D. Ebenezer, A. G. Morris, M. Krawczak, D. L. Thiselton, et al., A major marker for normal tension glaucoma: association with polymorphisms in the opa1 gene, *Hum. Genet.*, **110** (2002), 52–56.
27. M. A. Khaimi, Canaloplasty: A minimally invasive and maximally effective glaucoma treatment, *J. Ophthalmol.*, **2015**.
28. M. Bechmann, M. J. Thiel, B. Roesen, S. Ullrich, M. W. Ulbig, K. Ludwig, Central corneal thickness determined with optical coherence tomography in various types of glaucoma, *Br. J. Ophthalmol.*, **84** (2000), 1233–1237.
29. D. Ahram, W. Alward, M. Kuehn, The genetic mechanisms of primary angle closure glaucoma, *Eye.*, **29** (2015), 1251–1259.
30. R. Törnquist, Chamber depth in primary acute glaucoma, *Br. J. Ophthalmol.*, **40** (1956), 421.
31. H. S. Sugar, F. A. Barbour, Pigmentary glaucoma*: A rare clinical entity, *Am. J. Ophthalmol.*, **32** (1949), 90–92.
32. H. S. Sugar, Pigmentary glaucoma: A 25-year review, *Am. J. Ophthalmol.*, **62** (1966), 499–507.
33. R. Ritch, U. Schlötzer-Schrehardt, A. G. Konstas, Why is glaucoma associated with exfoliation syndrome?, *Prog. Retin. Eye Res.*, **22** (2003), 253–275.
34. J. L.-O. De, C. A. Girkin, Ocular trauma-related glaucoma., *Ophthalmol. Clin. North. Am.*, **15** (2002), 215–223.
35. E. Milder, K. Davis, Ocular trauma and glaucoma, *Int. Ophthalmol. Clin.*, **48** (2008), 47–64.
36. T. G. Papadaki, I. P. Zacharopoulos, L. R. Pasquale, W. B. Christen, P. A. Netland, C. S. Foster, Long-term results of ahmed glaucoma valve implantation for uveitic glaucoma, *Am. J. Ophthalmol.*, **144** (2007), 62–69.
37. H. C. Laganowski, M. G. K. Muir, R. A. Hitchings, Glaucoma and the iridocorneal endothelial syndrome, *Arch. Ophthalmol.*, **110** (1992), 346–350.
38. C. L. Ho, D. S. Walton, Primary congenital glaucoma: 2004 update, *J. Pediatr. Ophthalmol. Strabismus.*, **41** (2004), 271–288.
39. M. Erdurmuş, R. Yağcı, Ö. Atış, R. Karadağ, A. Akbaş, İ. F. Hepşen, Antioxidant status and oxidative stress in primary open angle glaucoma and pseudoexfoliative glaucoma, *Curr. Eye Res.*, **36** (2011), 713–718.
40. S. S. Hayreh, Neovascular glaucoma, *Prog. Retin. Eye Res.*, **26** (2007), 470–485.

41. D. A. Lee, E. J. Higginbotham, Glaucoma and its treatment: a review, *Am. J. Health. Syst. Pharm.*, **62** (2005), 691–699.
42. X. Wang, R. Khan, A. Coleman, Device-modified trabeculectomy for glaucoma, *Cochrane. Database Syst. Rev.*.
43. K. R. Sung, J. S. Kim, G. Wollstein, L. Folio, M. S. Kook, J. S. Schuman, Imaging of the retinal nerve fibre layer with spectral domain optical coherence tomography for glaucoma diagnosis, *Br. J. Ophthalmol.*, **95** (2011), 909–914.
44. M. E. Karlen, E. Sanchez, C. C. Schnyder, M. Sickenberg, A. Mermoud, Deep sclerectomy with collagen implant: medium term results, *Br. J. Ophthalmol.*, **83** (1999), 6–11.
45. J. Carrillo, L. Bautista, J. Villamizar, J. Rueda, M. Sanchez, D. Rueda, Glaucoma detection using fundus images of the eye, *2019 XXII Symposium on Image, Signal Processing and Artificial Vision (STSIVA)*, IEEE, 2019, 1–4.
46. N. Sengar, M. K. Dutta, R. Burget, M. Ranjoha, Automated detection of suspected glaucoma in digital fundus images, *2017 40th International Conference on Telecommunications and Signal Processing (TSP)*, IEEE, 2017, 749–752.
47. A. Poshtyar, J. Shanbehzadeh, H. Ahmadieh, Automatic measurement of cup to disc ratio for diagnosis of glaucoma on retinal fundus images, in *2013 6th International Conference on Biomedical Engineering and Informatics*, IEEE, 2013, 24–27.
48. F. Khan, S. A. Khan, U. U. Yasin, I. ul Haq, U. Qamar, Detection of glaucoma using retinal fundus images, in *The 6th 2013 Biomedical Engineering International Conference*, IEEE, 2013, 1–5.
49. H. Yamada, T. Akagi, H. Nakanishi, H. O. Ikeda, Y. Kimura, K. Suda, et al., Microstructure of peripapillary atrophy and subsequent visual field progression in treated primary open-angle glaucoma, *Ophthalmology*, **123** (2016), 542–551.
50. J. B. Jonas, Clinical implications of peripapillary atrophy in glaucoma, *Curr. Opin. Ophthalmol.*, **16** (2005), 84–88.
51. K. H. Park, G. Tomita, S. Y. Liou, Y. Kitazawa, Correlation between peripapillary atrophy and optic nerve damage in normal-tension glaucoma, *Ophthalmol.*, **103** (1996), 1899–1906.
52. F. A. Medeiros, L. M. Zangwill, C. Bowd, R. M. Vessani, R. Susanna Jr, R. N. Weinreb, Evaluation of retinal nerve fiber layer, optic nerve head, and macular thickness measurements for glaucoma detection using optical coherence tomography, *Am. J. Ophthalmol.*, **139** (2005), 44–55.
53. G. Wollstein, J. S. Schuman, L. L. Price, A. Aydin, P. C. Stark, E. Hertzmark, et al., Optical coherence tomography longitudinal evaluation of retinal nerve fiber layer thickness in glaucoma, *Arch. Ophthalmol.*, **123** (2005), 464–470.
54. M. Armaly, The optic cup in the normal eye: I. cup width, depth, vessel displacement, ocular tension and outflow facility, *Am. J. Ophthalmol.*, **68** (1969), 401–407.
55. M. Galdos, A. Bayon, F. D. Rodriguez, C. Mico, S. C. Sharma, E. Vecino, Morphology of retinal vessels in the optic disk in a göttingen minipig experimental glaucoma model, *Vet. Ophthalmol.*, **15** (2012), 36–46.

56. W. Zhou, Y. Yi, Y. Gao, J. Dai, Optic disc and cup segmentation in retinal images for glaucoma diagnosis by locally statistical active contour model with structure prior, *Comput. Math. Methods. Med.*, **2019**.
57. P. Sharma, P. A. Sample, L. M. Zangwill, J. S. Schuman, Diagnostic tools for glaucoma detection and management, *Surv. Ophthalmol.*, **53** (2008), S17–S32.
58. M. J. Greaney, D. C. Hoffman, D. F. Garway-Heath, M. Nakla, A. L. Coleman, J. Caprioli, Comparison of optic nerve imaging methods to distinguish normal eyes from those with glaucoma, *Invest. Ophthalmol. Vis. Sci.*, **43** (2002), 140–145.
59. R. Bock, J. Meier, L. G. Nyúl, J. Hornegger, G. Michelson, Glaucoma risk index: automated glaucoma detection from color fundus images, *Med. Image. Anal.*, **14** (2010), 471–481.
60. K. Chan, T.-W. Lee, P. A. Sample, M. H. Goldbaum, R. N. Weinreb, T. J. Sejnowski, Comparison of machine learning and traditional classifiers in glaucoma diagnosis, *IEEE Trans. Biomed. Eng.*, **49** (2002), 963–974.
61. N. Varachiu, C. Karanicolas, M. Ulieru, Computational intelligence for medical knowledge acquisition with application to glaucoma, in *Proceedings First IEEE International Conference on Cognitive Informatics*, IEEE, 2002, 233–238.
62. J. Yu, S. S. R. Abidi, P. H. Artes, A. McIntyre, M. Heywood, Automated optic nerve analysis for diagnostic support inglaucoma, in *CBMS'05.*, IEEE, 2005, 97–102.
63. R. Bock, J. Meier, G. Michelson, L. G. Nyúl and J. Hornegger, Classifying glaucoma with image-based features from fundus photographs, in *Joint Pattern Recognition Symposium.*, Springer, 2007, 355–364.
64. Y. Hatanaka, A. Noudo, C. Muramatsu, A. Sawada, T. Hara, T. Yamamoto, et al., Vertical cup-to-disc ratio measurement for diagnosis of glaucoma on fundus images, in *Medical Imaging 2010: Computer-Aided Diagnosis*, vol. 7624, International Society for Optics and Photonics, 2010, 76243C.
65. S. S. Abirami, S. G. Shoba, Glaucoma images classification using fuzzy min-max neural network based on data-core, *IJISME.*, **1** (2013), 9–15.
66. J. Liu, Z. Zhang, D. W. K. Wong, Y. Xu, F. Yin, J. Cheng, et al., Automatic glaucoma diagnosis through medical imaging informatics, *Journal of the American Medical Informatics Association*, **20** (2013), 1021–1027.
67. A. Almazroa, R. Burman, K. Raahemifar, V. Lakshminarayanan, Optic disc and optic cup segmentation methodologies for glaucoma image detection: A survey, *J. Ophthalmol.*, **2015**.
68. A. Dey, S. K. Bandyopadhyay, Automated glaucoma detection using support vector machine classification method, *J. Adv. Med. Med. Res.*, 1–12.
69. F. R. Silva, V. G. Vidotti, F. Cremasco, M. Dias, E. S. Gomi, V. P. Costa, Sensitivity and specificity of machine learning classifiers for glaucoma diagnosis using spectral domain oct and standard automated perimetry, *Arq. Bras. Oftalmol.*, **76** (2013), 170–174.
70. M. U. Akram, A. Tariq, S. Khalid, M. Y. Javed, S. Abbas, U. U. Yasin, Glaucoma detection using novel optic disc localization, hybrid feature set and classification techniques, *Australas. Phys. Eng. Sci. Med.*, **38** (2015), 643–655.

71. A. T. A. Al-Sammarraie, R. R. Jassem, T. K. Ibrahim, Mixed convection heat transfer in inclined tubes with constant heat flux, *Eur. J. Sci. Res.*, **97** (2013), 144–158.
72. M. R. K. Mookiah, U. R. Acharya, C. M. Lim, A. Petznick, J. S. Suri, Data mining technique for automated diagnosis of glaucoma using higher order spectra and wavelet energy features, *Knowl. Based. Syst.*, **33** (2012), 73–82.
73. C. Raja, N. Gangatharan, Glaucoma detection in fundal retinal images using trispectrum and complex wavelet-based features, *Eur. J. Sci. Res.*, **97** (2013), 159–171.
74. G. Lim, Y. Cheng, W. Hsu, M. L. Lee, Integrated optic disc and cup segmentation with deep learning, in *ICTAI.*, IEEE, 2015, 162–169.
75. K.-K. Maninis, J. Pont-Tuset, P. Arbeláez, L. Van Gool, Deep retinal image understanding, in *International conference on medical image computing and computer-assisted intervention*, Springer, 2016, 140–148.
76. B. Al-Bander, W. Al-Nuaimy, B. M. Williams, Y. Zheng, Multiscale sequential convolutional neural networks for simultaneous detection of fovea and optic disc, *Biomed. Signal Process Control.*, **40** (2018), 91–101.
77. A. Mitra, P. S. Banerjee, S. Roy, S. Roy, S. K. Setua, The region of interest localization for glaucoma analysis from retinal fundus image using deep learning, *Comput. Methods Programs Biomed.*, **165** (2018), 25–35.
78. S. S. Kruthiventi, K. Ayush, R. V. Babu, Deepfix: A fully convolutional neural network for predicting human eye fixations, *IEEE Trans. Image. Process.*, **26** (2017), 4446–4456.
79. M. Norouzifard, A. Nemati, A. Abdul-Rahman, H. GholamHosseini, R. Klette, A comparison of transfer learning techniques, deep convolutional neural network and multilayer neural network methods for the diagnosis of glaucomatous optic neuropathy, in *International Computer Symposium*, Springer, 2018, 627–635.
80. X. Sun, Y. Xu, W. Zhao, T. You, J. Liu, Optic disc segmentation from retinal fundus images via deep object detection networks, in *EMBC.*, IEEE, 2018, 5954–5957.
81. Z. Ghassabi, J. Shanbehzadeh, K. Nouri-Mahdavi, A unified optic nerve head and optic cup segmentation using unsupervised neural networks for glaucoma screening, in *EMBC.*, IEEE, 2018, 5942–5945.
82. J. H. Tan, S. V. Bhandary, S. Sivaprasad, Y. Hagiwara, A. Bagchi, U. Raghavendra, et al., Age-related macular degeneration detection using deep convolutional neural network, *Future Gener. Comput. Syst.*, **87** (2018), 127–135.
83. J. Zilly, J. M. Buhmann, D. Mahapatra, Glaucoma detection using entropy sampling and ensemble learning for automatic optic cup and disc segmentation, *Comput. Med. Imaging Graph.*, **55** (2017), 28–41.
84. J. Cheng, J. Liu, Y. Xu, F. Yin, D. W. K. Wong, N.-M. Tan, et al., Superpixel classification based optic disc and optic cup segmentation for glaucoma screening, *IEEE Trans. Med. Imaging*, **32** (2013), 1019–1032.
85. H. Ahmad, A. Yamin, A. Shakeel, S. O. Gillani, U. Ansari, Detection of glaucoma using retinal fundus images, in *iCREATE.*, IEEE, 2014, 321–324.

86. S. Kavitha, S. Karthikeyan, K. Duraiswamy, Neuroretinal rim quantification in fundus images to detect glaucoma, *IJCSNS.*, **10** (2010), 134–140.

87. Z. Zhang, B. H. Lee, J. Liu, D. W. K. Wong, N. M. Tan, J. H. Lim, et al., Optic disc region of interest localization in fundus image for glaucoma detection in argali, in *2010 5th IEEE Conference on Industrial Electronics and Applications*, IEEE, 2010, 1686–1689.

88. D. Welfer, J. Scharcanski, C. M. Kitamura, M. M. Dal Pizzol, L. W. Ludwig, D. R. Marinho, Segmentation of the optic disk in color eye fundus images using an adaptive morphological approach, *Computers Biol. Med.*, **40** (2010), 124–137.

89. H. Tjandrasa, A. Wijayanti, N. Suciati, Optic nerve head segmentation using hough transform and active contours, *Telkomnika*, **10** (2012), 531.

90. M. Tavakoli, M. Nazar, A. Golestaneh, F. Kalantari, Automated optic nerve head detection based on different retinal vasculature segmentation methods and mathematical morphology, in *NSS/MIC.*, IEEE, 2017, 1–7.

91. P. Bibiloni, M. González-Hidalgo, S. Massanet, A real-time fuzzy morphological algorithm for retinal vessel segmentation, *J. Real Time Image Process.*, **16** (2019), 2337–2350.

92. A. Agarwal, A. Issac, A. Singh, M. K. Dutta, Automatic imaging method for optic disc segmentation using morphological techniques and active contour fitting, in *2016 Ninth International Conference on Contemporary Computing (IC3)*, IEEE, 2016, 1–5.

93. S. Pal, S. Chatterjee, Mathematical morphology aided optic disk segmentation from retinal images, in *2017 3rd International Conference on Condition Assessment Techniques in Electrical Systems (CATCON)*, IEEE, 2017, 380–385.

94. L. Wang, A. Bhalerao, Model based segmentation for retinal fundus images, in *Scandinavian Conference on Image Analysis*, Springer, 2003, 422–429.

95. G. Deng, L. Cahill, An adaptive gaussian filter for noise reduction and edge detection, in *1993 IEEE conference record nuclear science symposium and medical imaging conference*, IEEE, 1993, 1615–1619.

96. K. A. Vermeer, F. M. Vos, H. G. Lemij, A. M. Vossepoel, A model based method for retinal blood vessel detection, *Comput. Biol. Med.*, **34** (2004), 209–219.

97. J. I. Orlando, E. Prokofyeva, M. B. Blaschko, A discriminatively trained fully connected conditional random field model for blood vessel segmentation in fundus images, *IEEE Trans. Biomed. Eng.*, **64** (2016), 16–27.

98. R. Ingle, P. Mishra, Cup segmentation by gradient method for the assessment of glaucoma from retinal image, *Int. J. Latest Trends. Eng. Technol.*, **4** (2013), 2540–2543.

99. G. D. Joshi, J. Sivaswamy, S. Krishnadas, Optic disk and cup segmentation from monocular color retinal images for glaucoma assessment, *IEEE Trans. Biomed. Eng.*, **30** (2011), 1192–1205.

100. W. W. K. Damon, J. Liu, T. N. Meng, Y. Fengshou, W. T. Yin, Automatic detection of the optic cup using vessel kinking in digital retinal fundus images, in *2012 9th IEEE International Symposium on Biomedical Imaging (ISBI)*, IEEE, 2012, 1647–1650.

101. D. Finkelstein, Kinks, *J. Math. Phys.*, **7** (1966), 1218–1225.

102. Y. Xu, L. Duan, S. Lin, X. Chen, D. W. K. Wong, T. Y. Wong, et al., Optic cup segmentation for glaucoma detection using low-rank superpixel representation, in *International Conference on Medical Image Computing and Computer-Assisted Intervention*, Springer, 2014, 788–795.

103. Y. Xu, J. Liu, S. Lin, D. Xu, C. Y. Cheung, T. Aung, et al., Efficient optic cup detection from intra-image learning with retinal structure priors, in *International Conference on Medical Image Computing and Computer-Assisted Intervention*, Springer, 2012, 58–65.

104. M. A. Aslam, M. N. Salik, F. Chughtai, N. Ali, S. H. Dar, T. Khalil, Image classification based on mid-level feature fusion, in *2019 15th International Conference on Emerging Technologies (ICET)*, IEEE, 2019, 1–6.

105. N. Ali, K. B. Bajwa, R. Sablatnig, S. A. Chatzichristofis, Z. Iqbal, M. Rashid, et al., A novel image retrieval based on visual words integration of sift and surf, *PloS. one.*, **11** (2016), e0157428.

106. C.-Y. Ho, T.-W. Pai, H.-T. Chang, H.-Y. Chen, An atomatic fundus image analysis system for clinical diagnosis of glaucoma, in *2011 International Conference on Complex, Intelligent, and Software Intensive Systems*, IEEE, 2011, 559–564.

107. H.-T. Chang, C.-H. Liu, T.-W. Pai, Estimation and extraction of b-cell linear epitopes predicted by mathematical morphology approaches, *J. Mol. Recognit.*, **21** (2008), 431–441.

108. D. Wong, J. Liu, J. Lim, N. Tan, Z. Zhang, S. Lu, et al., Intelligent fusion of cup-to-disc ratio determination methods for glaucoma detection in argali, in *2009 Annual International Conference of the IEEE Engineering in Medicine and Biology Society*, IEEE, 2009, 5777–5780.

109. F. Yin, J. Liu, D. W. K. Wong, N. M. Tan, C. Cheung, M. Baskaran, et al., Automated segmentation of optic disc and optic cup in fundus images for glaucoma diagnosis, in *2012 25th IEEE international symposium on computer-based medical systems (CBMS)*, IEEE, 2012, 1–6.

110. S. Chandrika, K. Nirmala, Analysis of cdr detection for glaucoma diagnosis, *IJERA.*, **2** (2013), 23–27.

111. N. Annu, J. Justin, Automated classification of glaucoma images by wavelet energy features, *IJERA.*, **5** (2013), 1716–1721.

112. H. Fu, J. Cheng, Y. Xu, D. W. K. Wong, J. Liu, X. Cao, Joint optic disc and cup segmentation based on multi-label deep network and polar transformation, *IEEE Trans. Med. Imaging.*, **37** (2018), 1597–1605.

113. P. K. Dhar, T. Shimamura, Blind svd-based audio watermarking using entropy and log-polar transformation, *JISA.*, **20** (2015), 74–83.

114. D. Wong, J. Liu, J. Lim, H. Li, T. Wong, Automated detection of kinks from blood vessels for optic cup segmentation in retinal images, in *Medical Imaging 2009: Computer-Aided Diagnosis*, vol. 7260, International Society for Optics and Photonics, 2009, 72601J.

115. A. Murthi, M. Madheswaran, Enhancement of optic cup to disc ratio detection in glaucoma diagnosis, in *2012 International Conference on Computer Communication and Informatics*, IEEE, 2012, 1–5.

116. N. E. A. Khalid, N. M. Noor, N. M. Ariff, Fuzzy c-means (fcm) for optic cup and disc segmentation with morphological operation, *Procedia. Comput. Sci.*, **42** (2014), 255–262.

117. H. A. Nugroho, W. K. Oktoeberza, A. Erasari, A. Utami, C. Cahyono, Segmentation of optic disc and optic cup in colour fundus images based on morphological reconstruction, in *2017 9th International Conference on Information Technology and Electrical Engineering (ICITEE)*, IEEE, 2017, 1–5.

118. L. Zhang, M. Fisher, W. Wang, Retinal vessel segmentation using multi-scale textons derived from keypoints, *Comput. Med. Imaging Graph.*, **45** (2015), 47–56.

119. X. Li, B. Aldridge, R. Fisher, J. Rees, Estimating the ground truth from multiple individual segmentations incorporating prior pattern analysis with application to skin lesion segmentation, in *2011 IEEE International Symposium on Biomedical Imaging: From Nano to Macro*, IEEE, 2011, 1438–1441.

120. M. M. Fraz, P. Remagnino, A. Hoppe, S. Velastin, B. Uyyanonvara, S. Barman, A supervised method for retinal blood vessel segmentation using line strength, multiscale gabor and morphological features, in *2011 IEEE International Conference on Signal and Image Processing Applications (ICSIPA)*, IEEE, 2011, 410–415.

121. M. Niemeijer, J. Staal, B. van Ginneken, M. Loog, M. D. Abramoff, Comparative study of retinal vessel segmentation methods on a new publicly available database, in *Medical imaging 2004: Image processing*, vol. 5370, International Society for Optics and Photonics, 2004, 648–656.

122. J. Y. Choi, T. K. Yoo, J. G. Seo, J. Kwak, T. T. Um, T. H. Rim, Multi-categorical deep learning neural network to classify retinal images: a pilot study employing small database, *PloS one*, **12**.

123. L. Zhang, M. Fisher, W. Wang, Comparative performance of texton based vascular tree segmentation in retinal images, in *2014 IEEE International Conference on Image Processing (ICIP)*, IEEE, 2014, 952–956.

124. A. Septiarini, A. Harjoko, R. Pulungan, R. Ekantini, Automated detection of retinal nerve fiber layer by texture-based analysis for glaucoma evaluation, *Healthc. Inform. Res.*, **24** (2018), 335–345.

125. B. S. Kirar, D. K. Agrawal, Computer aided diagnosis of glaucoma using discrete and empirical wavelet transform from fundus images, *IET Image Process.*, **13** (2018), 73–82.

126. K. Nirmala, N. Venkateswaran, C. V. Kumar, J. S. Christobel, Glaucoma detection using wavelet based contourlet transform, in *2017 International Conference on Intelligent Computing and Control (I2C2)*, IEEE, 2017, 1–5.

127. A. A. G. Elseid, A. O. Hamza, Glaucoma detection using retinal nerve fiber layer texture features, *J. Clin. Eng.*, **44** (2019), 180–185.

128. M. Claro, L. Santos, W. Silva, F. Araújo, N. Moura, A. Macedo, Automatic glaucoma detection based on optic disc segmentation and texture feature extraction, *CLEI Electron. J.*, **19** (2016), 5.

129. L. Abdel-Hamid, Glaucoma detection from retinal images using statistical and textural wavelet features, *J. Digit Imaging.*, 1–8.

130. S. Maetschke, B. Antony, H. Ishikawa, G. Wollstein, J. Schuman, R. Garnavi, A feature agnostic approach for glaucoma detection in oct volumes, *PloS. one.*, **14** (2019), e0219126.

131. D. C. Hood, A. S. Raza, On improving the use of oct imaging for detecting glaucomatous damage, *Br. J. Ophthalmol.*, **98** (2014), ii1–ii9.

132. D. C. Hood, Improving our understanding, and detection, of glaucomatous damage: an approach based upon optical coherence tomography (oct), *Prog.Retin. Eye Res.*, **57** (2017), 46–75.

133. H. S. Basavegowda, G. Dagnew, Deep learning approach for microarray cancer data classification, *CAAI Trans. Intell. Technol.*, **5** (2020), 22–33.

134. X. Chen, Y. Xu, D. W. K. Wong, T. Y. Wong, J. Liu, Glaucoma detection based on deep convolutional neural network, in *2015 37th annual international conference of the IEEE engineering in medicine and biology society (EMBC)*, IEEE, 2015, 715–718.

135. U. T. Nguyen, A. Bhuiyan, L. A. Park, K. Ramamohanarao, An effective retinal blood vessel segmentation method using multi-scale line detection, *Pattern Recognit.*, **46** (2013), 703–715.

136. J. H. Tan, U. R. Acharya, S. V. Bhandary, K. C. Chua, S. Sivaprasad, Segmentation of optic disc, fovea and retinal vasculature using a single convolutional neural network, *J. Comput. Sci.*, **20** (2017), 70–79.

137. Y. Chai, H. Liu, J. Xu, Glaucoma diagnosis based on both hidden features and domain knowledge through deep learning models, *Knowl. Based Syst.*, **161** (2018), 147–156.

138. A. Pal, M. R. Moorthy, A. Shahina, G-eyenet: A convolutional autoencoding classifier framework for the detection of glaucoma from retinal fundus images, in *2018 25th IEEE International Conference on Image Processing (ICIP)*, IEEE, 2018, 2775–2779.

139. R. Asaoka, M. Tanito, N. Shibata, K. Mitsuhashi, K. Nakahara, Y. Fujino, et al., Validation of a deep learning model to screen for glaucoma using images from different fundus cameras and data augmentation, *Ophthalmol. Glaucoma.*, **2** (2019), 224–231.

140. X. Chen, Y. Xu, S. Yan, D. W. K. Wong, T. Y. Wong, J. Liu, Automatic feature learning for glaucoma detection based on deep learning, in *International Conference on Medical Image Computing and Computer-Assisted Intervention*, Springer, 2015, 669–677.

141. A. Singh, S. Sengupta, V. Lakshminarayanan, Glaucoma diagnosis using transfer learning methods, in *Applications of Machine Learning*, vol. 11139, International Society for Optics and Photonics, 2019, 111390U.

142. S. Maheshwari, V. Kanhangad, R. B. Pachori, Cnn-based approach for glaucoma diagnosis using transfer learning and lbp-based data augmentation, *arXiv. preprint*.

143. S. Sengupta, A. Singh, H. A. Leopold, T. Gulati, V. Lakshminarayanan, Ophthalmic diagnosis using deep learning with fundus images–a critical review, *Artif. Intell. Med.*, **102** (2020), 101758.

144. U. Raghavendra, H. Fujita, S. V. Bhandary, A. Gudigar, J. H. Tan, U. R. Acharya, Deep convolution neural network for accurate diagnosis of glaucoma using digital fundus images, *Inf. Sci.*, **441** (2018), 41–49.

145. R. Asaoka, H. Murata, A. Iwase, M. Araie, Detecting preperimetric glaucoma with standard automated perimetry using a deep learning classifier, *Ophthalmol.*, **123** (2016), 1974–1980.

146. Z. Li, Y. He, S. Keel, W. Meng, R. T. Chang, M. He, Efficacy of a deep learning system for detecting glaucomatous optic neuropathy based on color fundus photographs, *Ophthalmol.*, **125** (2018), 1199–1206.

147. V. V. Raghavan, V. N. Gudivada, V. Govindaraju, C. R. Rao, Cognitive computing: Theory and applications, *Elsevier.*, 2016.

148. J. Sivaswamy, S. Krishnadas, G. D. Joshi, M. Jain, A. U. S. Tabish, Drishti-gs: Retinal image dataset for optic nerve head (onh) segmentation, in *2014 IEEE 11th international symposium on biomedical imaging (ISBI)*, IEEE, 2014, 53–56.

149. A. Chakravarty, J. Sivaswamy, Glaucoma classification with a fusion of segmentation and image-based features, in *2016 IEEE 13th international symposium on biomedical imaging (ISBI)*, IEEE, 2016, 689–692.

150. E. Decencière, X. Zhang, G. Cazuguel, B. Lay, B. Cochener, C. Trone, et al., Feedback on a publicly distributed image database: The messidor database, *Image Analys. Stereol.*, **33** (2014), 231–234.

151. A. Allam, A. Youssif, A. Ghalwash, Automatic segmentation of optic disc in eye fundus images: a survey, *ELCVIA*, **14** (2015), 1–20.

152. P. Porwal, S. Pachade, R. Kamble, M. Kokare, G. Deshmukh, V. Sahasrabuddhe, et al., Indian diabetic retinopathy image dataset (idrid): A database for diabetic retinopathy screening research, *Data*, **3** (2018), 25.

153. F. Calimeri, A. Marzullo, C. Stamile, G. Terracina, Optic disc detection using fine tuned convolutional neural networks, in *2016 12th International Conference on Signal-Image Technology & Internet-Based Systems (SITIS)*, IEEE, 2016, 69–75.

154. M. N. Reza, Automatic detection of optic disc in color fundus retinal images using circle operator, *Biomed. Signal. Process. Control.*, **45** (2018), 274–283.

155. Z. Zhang, F. S. Yin, J. Liu, W. K. Wong, N. M. Tan, B. H. Lee, et al., Origa-light: An online retinal fundus image database for glaucoma analysis and research, in *2010 Annual International Conference of the IEEE Engineering in Medicine and Biology*, IEEE, 2010, 3065–3068.

156. Z. Zhang, J. Liu, F. Yin, B.-H. Lee, D. W. K. Wong, K. R. Sung, Achiko-k: Database of fundus images from glaucoma patients, in *2013 IEEE 8th Conference on Industrial Electronics and Applications (ICIEA)*, IEEE, 2013, 228–231.

157. F. Yin, J. Liu, D. W. K. Wong, N. M. Tan, B. H. Lee, J. Cheng, et al., Achiko-i retinal fundus image database and its evaluation on cup-to-disc ratio measurement, in *2013 IEEE 8th Conference on Industrial Electronics and Applications (ICIEA)*, IEEE, 2013, 224–227.

158. F. Fumero, S. Alayón, J. L. Sanchez, J. Sigut, M. Gonzalez-Hernandez, Rim-one: An open retinal image database for optic nerve evaluation, in *2011 24th international symposium on computer-based medical systems (CBMS)*, IEEE, 2011, 1–6.

159. J. Lowell, A. Hunter, D. Steel, A. Basu, R. Ryder, E. Fletcher, et al., Optic nerve head segmentation, *IEEE Trans. Med. Imaging.*, **23** (2004), 256–264.

160. C. C. Sng, L.-L. Foo, C.-Y. Cheng, J. C. Allen Jr, M. He, G. Krishnaswamy, et al., Determinants of anterior chamber depth: the singapore chinese eye study, *Ophthalmol.*, **119** (2012), 1143–1150.

161. Z. Zhang, J. Liu, C. K. Kwoh, X. Sim, W. T. Tay, Y. Tan, et al., Learning in glaucoma genetic risk assessment, in *2010 Annual International Conference of the IEEE Engineering in Medicine and Biology*, IEEE, 2010, 6182–6185.

162. D. Wong, J. Liu, J. Lim, X. Jia, F. Yin, H. Li, et al., Level-set based automatic cup-to-disc ratio determination using retinal fundus images in argali, in *2008 30th Annual International Conference of the IEEE Engineering in Medicine and Biology Society*, IEEE, 2008, 2266–2269.

163. T. Ge, L. Cui, B. Chang, Z. Sui, F. Wei, M. Zhou, Seri: A dataset for sub-event relation inference from an encyclopedia, in *CCF International Conference on Natural Language Processing and Chinese Computing*, Springer, 2018, 268–277.

164. M. Haloi, Improved microaneurysm detection using deep neural networks, *arXiv. preprint.*.

165. B. Antal, A. Hajdu, An ensemble-based system for automatic screening of diabetic retinopathy, *Knowl. Based Syst.*, **60** (2014), 20–27.

166. J. Nayak, R. Acharya, P. S. Bhat, N. Shetty, T.-C. Lim, Automated diagnosis of glaucoma using digital fundus images, *J. Med. Syst.*, **33** (2009), 337.

167. J. V. Soares, J. J. Leandro, R. M. Cesar, H. F. Jelinek, M. J. Cree, Retinal vessel segmentation using the 2-d gabor wavelet and supervised classification, *IEEE Trans. Med. Imaging.*, **25** (2006), 1214–1222.

168. S. Kankanahalli, P. M. Burlina, Y. Wolfson, D. E. Freund, N. M. Bressler, Automated classification of severity of age-related macular degeneration from fundus photographs, *Invest. Ophthalmol. Vis. Sci.*, **54** (2013), 1789–1796.

169. K. Prasad, P. Sajith, M. Neema, L. Madhu, P. Priya, Multiple eye disease detection using deep neural network, in *TENCON 2019-2019 IEEE Region 10 Conference (TENCON)*, IEEE, 2019, 2148–2153.

AIMS Press